COO-3258-1 November, 1973

ENERGETIC NEUTRON SPECTROMETRY

by

Richard Madey and Frank M. Waterman

FINAL REPORT

Prepared For

THE U. S. ATOMIC ENERGY COMMISSION

for the period from

1 December 1967 through 31 March 1972

under

Contracts AT(30-1)-3914 and AT(11-1)-3258

with

Clarkson College of Technology

Potsdam, New York 13676

DISCLAIMER

Blank Page

Abstract

A research program in energetic-neutron spectrometry was carried out under Contracts AT(30-1)-3914 and AT(11-1)-3258 with Clarkson College of Technology during the period from 1 December 1967 through 31 March 1972. Accomplishments under this program include the development of a self-contained time-of-flight spectrometer for neutrons from 1 to 500 MeV and the measurement of neutron spectra from a thick target. Early developmental work was conducted with 14 MeV neutrons at the National Research Council, Ottawa, Canada. Later, measurements at higher energies were made at the 184-inch cyclotron of the Lawrence Berkeley Laboratory. These include the measurement of 220 MeV neutrons from stripping 447 MeV deuterons on beryllium and the measurement of neutron spectra from 740 MeV proton bombardment of a thick uranium target.

Basically, the spectrometer measures the time-of-flight of a neutron scattered between two scintillation counters. The intrinsic time dispersion of the system is 2.2 nanoseconds (fwhm) with a $2\frac{1}{2}$ inch diameter by $2\frac{1}{2}$ inch high first detector and a 9 inch diameter by 8 inch thick second detector. For a flight path of 4 meters, the energy resolution of the spectrometer varies from about 2×10^{-5} at 10 MeV to 8×10^{-7} at 500 MeV. Background from neutron-carbon interactions is determined from separate spectral measurements with first detectors differing

significantly in their relative hydrogen-carbon composition. Measurements with 14 MeV neutrons confirm the resolution and efficiency of the spectrometer at low energies. Measurements at 220 MeV verify the resolution of the spectrometer at this energy and demonstrate the technique for subtracting the carbon background.

Neutron spectra from 740 MeV proton bombardment of a 30-cm thick uranium target were measured from 20 to 500 MeV at 50 degrees and from 5 to 140 MeV at 130 degrees with respect to the proton beam at LBL. The results are compared with a Monte Carlo calculation of the neutron cascade-evaporation spectrum. While the shapes of the measured and calculated spectra are in general agreement, this comparison shows that the intranuclear cascade model underestimates the production of cascade neutrons at wide angles; furthermore, this comparison shows that this discrepancy increases with increasing angle of emission.

TABLE OF CONTENTS

LIST OF TABLES

Blank Page

LIST OF FIGURES

BIBLIOGRAPHY OF PAPERS AND REPORTS GENERATED UNDER CONTRACTS AT(30-1)-3914 and AT(11-1)-3258

1. Richard Madey, A Time-of-Flight Spectrometer for Neutrons from 10 to 100 MeV, Bull, Am. Phys. Soc. 13 (1), 51 (January 1968); also designated as NYO-3914-1.

2. Richard Madey, A Spectrometer for Neutrons from 10 to 100 MeV, Proceedings of the International Symposium on Nuclear Electronics and Radioprotection, Toulouse, France, (March 1968); also designated as NYO-3914-2.

3. Richard Madey, A Spectrometer for Energetic Neutrons, IEEE Transactions on Nuclear Science NS-15 (3), 426-438 (June 1968); also designated as NYO-3914-4.

4. David H. Osborn and Richard Madey, Neutron Spectrometer Performance at 14 MeV, Bull. Am. Phys. Soc. 14 (12), 1214 (1969).

5. David H. Osborn and Richard Madey, Neutron Spectrometer Performance at 14 MeV, CONF-691101, Proceedings of the Second International Conference on Accelerator Dosimetry and Experience Stanford Linear Accelerator Center, Stanford, California (5-7 November 1969).

6. F. M. Waterman, D. H. Osborn, P. J. McNulty, and R. Madey, Neutron Spectrometer Studies at 14 MeV, Bull. Am. Phys. Soc. 15 (4), 599 (April 1970).

7. NYO-3914-3, Progress Report No. 1, (for period from 1 December 1967 to 14 August 1968), An Energetic-Neutron Spectrometer, Richard Madey (August 1968).

8. Richard Madey, A Time-of-Flight Spectrometer for Energetic Neutrons, Shielding Division Informal Session, American Nuclear Society (June 1968); also designated as NYO-3914-5.

9. NYO-3914-6, Progress Report No. 2, (for period from 15 August 1968 to 15 September 1969), Energetic-Neutron Spectrometry, Richard Madey, Peter McNulty, David Osborn, and Frank Waterman (September 1969).

10. NYO-3914-7, Progress Report No. 3 (for period from 16 September 1969 to 14 August 1970), Energetic-Neutron Spectrometry, Richard Madey and Frank Waterman (August 1970).

11. Alan R. Baldwin, A. Gated Pulse-Shape Discrimination System for High Data Acquisition Rates, M. S. Thesis, Clarkson College of Technology (June 1971).

12. Frank M. Waterman, High-Energy Neutrons Produced by 740 MeV Protons on Uranium, Ph.D. Dissertation, Clarkson College of Technology (May 1973).

1. INTRODUCTION

This report describes the research accomplishments in the program of energetic-neutron spectrometry carried out under contract AT(30-1)-3914 with Clarkson College of Technology during the period from 1 December 1967 to 31 March 1972.

The objectives of this work were to develop a self-contained time-of-flight spectrometer for measuring neutron spectra in the energy region from about 10 to 100 MeV and to make measurements of energetic-neutron spectra at particle accelerators. Both of these objectives were achieved; in fact, as the work progressed it was possible to extend the energy region of the spectrometer down to 1 MeV and up to 500 MeV. Section 2 of this report describes the spectrometer and the spectrometer performance in measuring monoenergetic neutrons at 14 and 220 MeV. Section 3 describes measurements of neutron spectra from 740 MeV proton bombardment of a thick uranium target at the 184-inch cyclotron of the Lawrence Berkeley Laboratory. Measurements were made from 20 to 500 MeV at 50 degrees and from 5 to 140 MeV at 130 degrees with respect to the proton beam.

2. THE NEUTRON TIME-OF-FLIGHT SPECTROMETER

2-1. Introduction

The purpose of Section 2 is to describe the design and performance characteristics of the time-of-flight spectrometer for neutrons from 1 to 500 MeV. Basically, the spectrometer measures the time-of-flight of neutrons scattered between two scintillation counters. The low-energy limit of the spectrometer is defined by the ability to detect recoil protons in the first detector with 100 percent efficiency. The high-energy limit occurs in practice when the background becomes significant from the neutron-proton inelastic scattering reactions:

$$n + p \rightarrow n + p + \pi^{o}$$

$$n + p \rightarrow n + n + \pi^{+}$$

Below 500 MeV, the cross sections for these n-p inelastic interactions are small relative to the total n-p cross section; hence, the spectrometer can be used for most applications to detect neutrons with energies up to about 500 MeV.

Earlier versions of this spectrometer have been reported previously by Madey (1968 a, b, c) and Osborn and Madey (1969 a, b) for the energy region from 10 to 100 MeV. The work done since these previous reports has extended the energy region of the spectro-

meter down to 1 MeV and up to about 500 MeV, and has included several advances and modifications: (1) development of an electronic scheme to eliminate blocking in the time-to-amplitude converter, (2) development of a technique for subtracting the background from neutron-carbon interactions, (3) design and introduction of a large detector to improve the spectrometer efficiency, (4) introduction of constant-fraction timing discriminators to improve the energy resolution of the spectrometer, and (5) development of a technique to eliminate blocking in the pulse-shape-discrimination system.

2-2. Principle

The neutron spectrometer consists of the four scintillation counters D1, D2, A1, A2, which are shown schematically in Fig. 1. The principle of the spectrometer requires an incident neutron to scatter elastically from a hydrogen nucleus in the D1 scintillator. The scattered neutron must then travel over a fixed flight path X and interact in the D2 scintillator. The time-of-flight t of the scattered neutron is measured by the time interval between the scintillation pulses from the neutron interactions in the D1 and

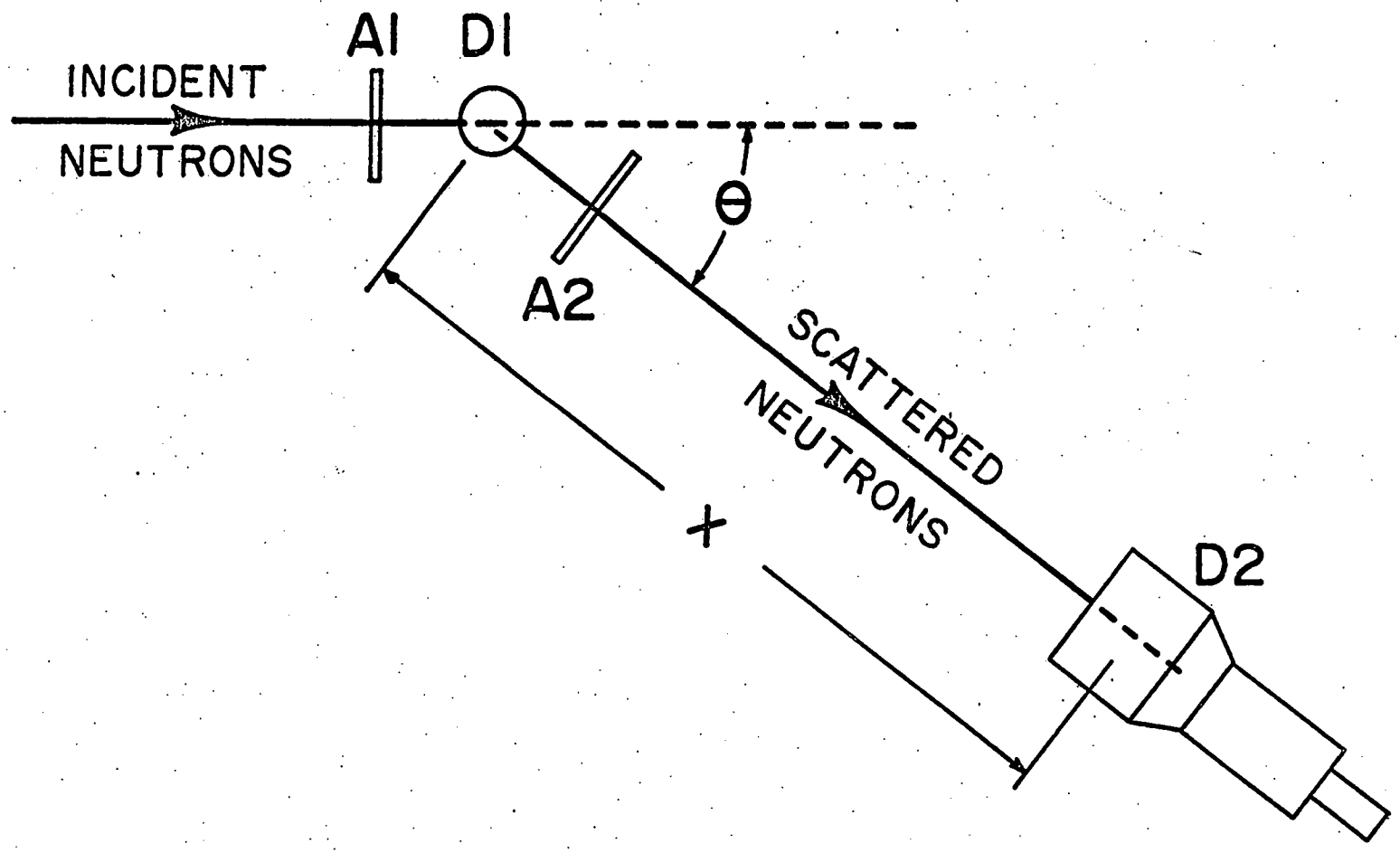

FIG. 1 A schematic diagram of the time-of-flight spectrometer.

D2 detectors. The purpose of the A1 and A2 scintillation detectors is to veto events produced by charged particles in the incident and scattered neutron beams.

The kinetic energy T' of a scattered neutron is determined from the measured time-of-flight t and the flight path X by the relativistic expression

$$T' = M_n [1/ (1-X^2/c^2t^2)^{1/2} - 1] \qquad (1)$$

where M_n is the neutron rest mass in MeV, and c is the speed of light.

The D2 detector is positioned at an angle Θ with respect to the direction of the incident neutrons at the D1 detector. Since the position of the D2 detector defines the neutron scattering angle Θ, the incident neutron kinetic energy T is determined from the kinematic expression

$$T = 2M/[(1 + 2M/T') \cos^2\Theta - 1] \qquad (2)$$

where M is the nucleon rest mass. Here the assumption has been made that the neutron and proton rest masses are equal.

2-3. Apparatus

2-3.1 Detectors

The large scintillator shown in Fig. 2 serves as the D2 detector for measurements above about 15 MeV. This detector

consists of a 9 inch diameter by 8 inch thick NE-102 plastic scintillator† coupled to an Amperex 58 DVP photomultiplier by means of a tapered lucite light-pipe. An aluminum housing combines the photomultiplier base, the photomultiplier, the magnetic shield, the light-pipe, and the scintillator into a single unit. Using a computer program written by Kurz (1964), we have calculated the efficiency of this scintillator for detecting the scattered neutrons. Crabb et al. (1967), Brady et al. (1968), and Young et al. (1969) have reported efficiency measurements for neutron energies from 10 to 170 MeV in agreement with the values obtained from the Kurz program; in addition, Kurz has compared his calculation with the prior measurements of Wiegand et al. (1962). Figure 3 is a plot of the detection efficiency of the large D2 scintillator for neutron energies from 10 to 300 MeV for several detector thresholds. The dashed portions of the smooth curves designate regions with rapid, and sometimes abrupt, changes in the computed efficiency. As can be seen from this figure, it is possible to attain

---

†Nuclear Enterprises, Inc., 935 Terminal Way, San Carlos, California

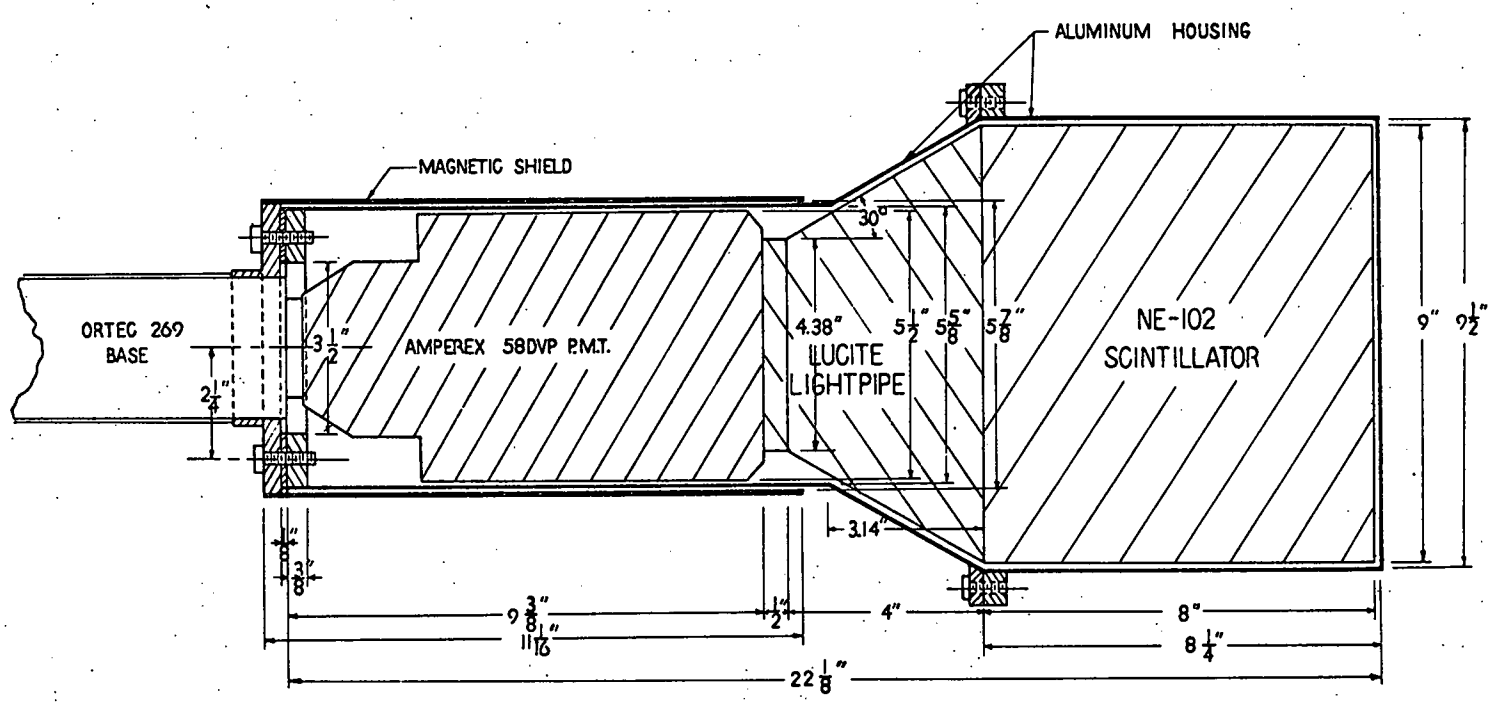

FIG. 2 Construction of the 9 inch diameter by 8 inch thick D2 detector.

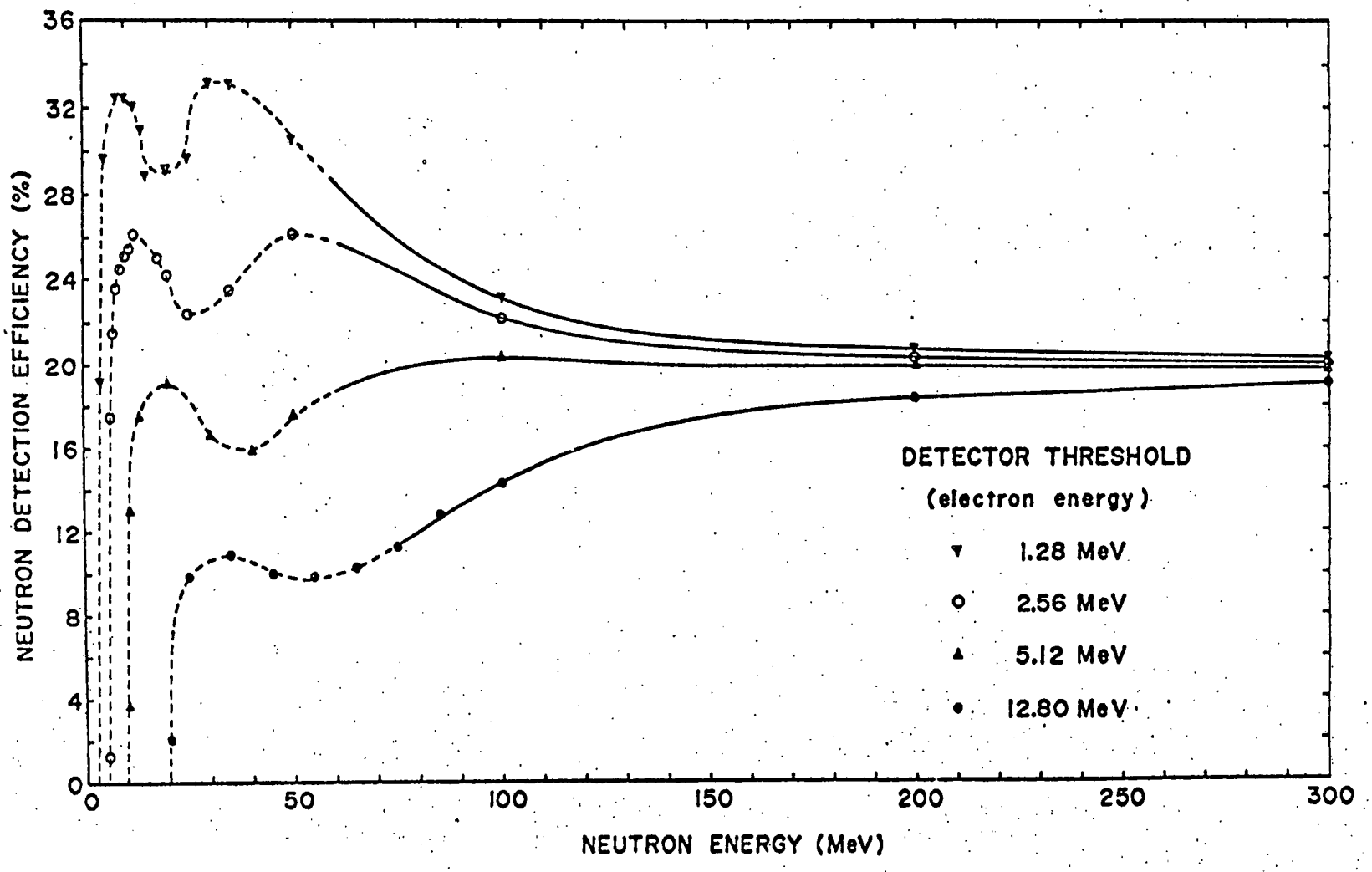

FIG. 3 The neutron detection efficiency predicted by the Kurz efficiency program for a 9 inch diameter by 8 inch thick plastic scintillator as a function of the neutron energy for electron energy thresholds of 1.28, 2.56, 5.12, and 12.80 MeV.

a detection efficiency of approximately 20 percent or better for neutron energies above 10 MeV.

In conjunction with this large D2 detector, we have most frequently used a $2\frac{1}{2}$ inch diameter by $2\frac{1}{2}$ inch high scintillator for the D1 detector; however, scintillators as large as 4 inch diameter by 4 inch high have been used for some measurements. The A1 and A2 anticoincidence detectors consist of $\frac{1}{4}$ inch thick slabs of NE-102 plastic scintillator: 4 inches by 4 inches for A1 and 6 inches by 6 inches for A2. The A2 scintillator is bonded to an adiabatic lucite light-pipe $1\frac{1}{2}$ inches high.

Smaller detectors have been used for neutron energies below 15 MeV; for example, we have measured a neutron spectrum from 1 to 15 MeV with a 1 inch diameter by 1 inch high NE-102 plastic scintillator for the D1 detector and a 4 inch diameter by 2 inch thick NE-102 plastic scintillator for the D2 detector.

It is well known that the response of organic scintillators is linear for electrons but not for protons. The discriminator bias of each of the detectors is calibrated in units of equivalent-electron energy to provide a linear scale for adjusting the discriminator bias to a particular recoil proton energy. The response of protons in NE-102 scintillator in units of equivalent-electron energy

can be obtained from the calculated response of Gooding and Pugh (1960, 1961).

The peaks of the Compton spectra of the 0.51 and 1.28 MeV gamma-rays from sodium-22 and the 2.62 MeV gamma-rays from thorium-228 serve as calibration points for calibration of the discriminator biases. Since large scintillators are used in this spectrometer, it is necessary to have a calibration point, such as the peak of a Compton spectrum, which is insensitive to the pulse-height resolution of the detector. The Compton peak is taken to corrspond to the maximum Compton electron energy produced by the associated gamma-ray.

2-3.2 Electronics

The electronic apparatus shown in Fig. 4 is designed to measure (1) the neutron time-of-flight spectrum, (2) the time-of-flight spectrum of accidental coincidences, (3) the number of D1 events vetoed, and (4) the number of D1 events accidentally vetoed. For clarity in identification, the group of components performing each of these functions have been designated coincidence channels 1, 2, 3, and 4, respectively.

Coincidence channel 1 measures the neutron time-of-flight spectrum. The time-to-amplitude converter (TAC) converts

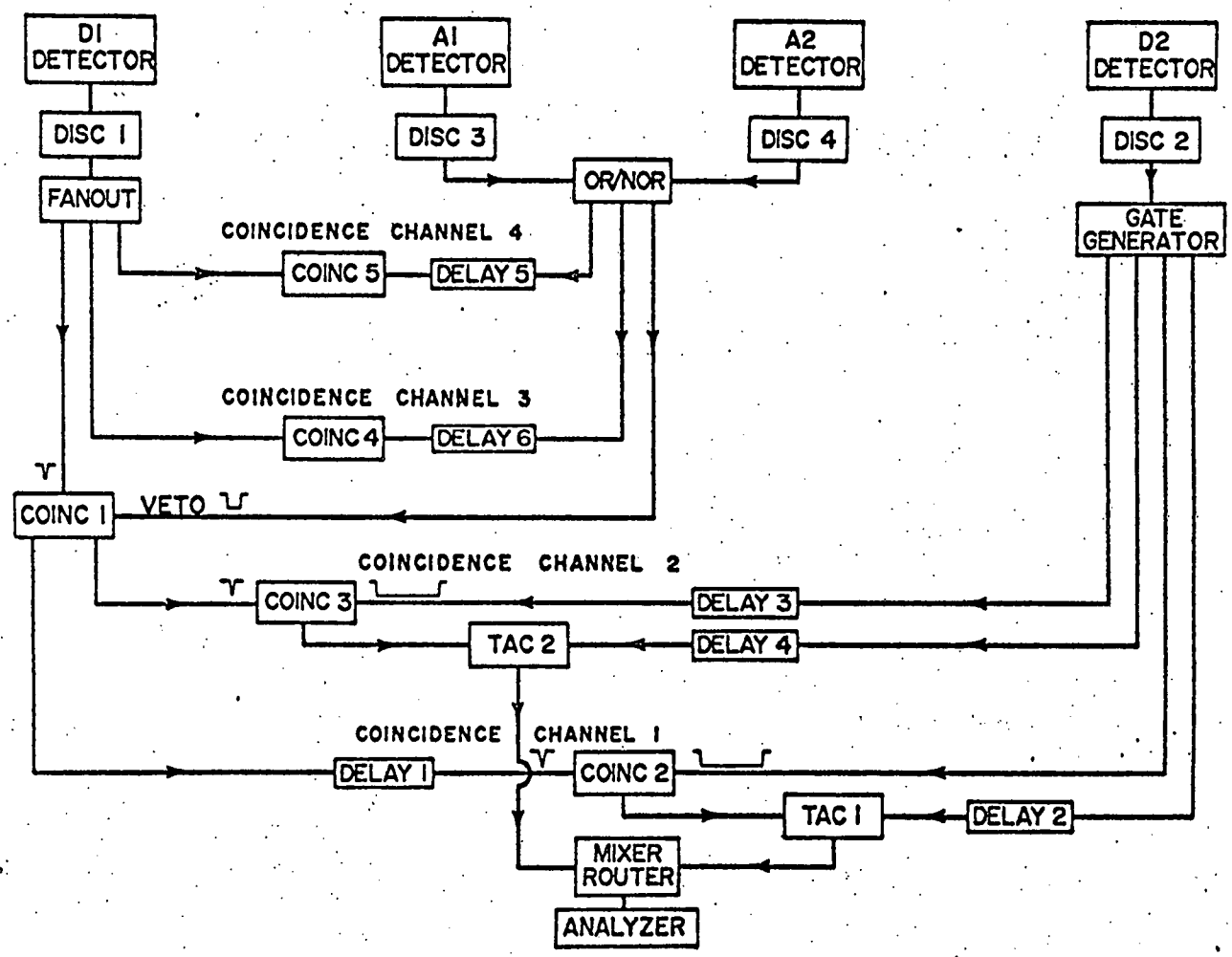

FIG. 4 Block diagram of the electronic system.

the time interval between scintillation pulses in the D1 and D2 detectors into a pulse amplitude which is stored in a multi-channel analyzer. In an early measurement, Osborn and Madey (1969a) encountered blocking losses in the TAC unit when the TAC received a start signal from each scintillation pulse in the D1 detector. To avoid these losses, we have introduced a means for rejecting most of the unwanted D1 scintillation pulses since only a small fraction of the D1 pulses are produced by neutrons that scatter into the D2 detector. The criterion for selection of a D1 start pulse is that a D2 pulse must occur within a preselected time interval after a D1 pulse. This selection is made by delaying the D1 pulse (by inserting DELAY 1) such that the D2 pulse precedes the D1 pulse to the coincidence module (COINC 2). A coincidence (in COINC 2) between events in the D1 and D2 detectors generates the start signal for TAC 1. The stop signal for TAC 1 is a delayed pulse from the same D2 event that produced the coincidence. In this manner, we have achieved a large increase in the count-rate capability of the spectrometer without incurring blocking losses in the TAC.

The GATE GENERATOR increases the D2 pulse duration to approximately three times the range of flight-times in the

spectrum. The range of flight-times, which includes the gamma-ray peak and the neutron spectrum, is simply the difference between the gamma-ray time-of-flight and the time-of-flight of the lowest neutron energy permitted by the D1 detector bias. This gate-width will insure that there are regions of the spectrum composed of only accidental coincidences so that the background of accidental coincidences can be determined.

Coincidence channel 2 measures the time-of-flight spectrum of accidental coincidences. The D2 pulse was delayed (by inserting DELAY 3) to insure that the D1 and D2 pulses from a real event could not produce a coincidence (in COINC 3); hence, only accidental or random coincidences occur. This spectrum was measured simultaneously with the neutron time-of-flight spectrum and stored in a separate portion of the analyzer memory. This spectrum is useful in determining the background of accidental coincidences in the neutron time-of-flight spectrum, particularly if the accidental coincidences have a periodic structure which can occur as a result of the radio-frequency structure of an accelerator beam.

Events resulting from charged particles in the incident

and scattered neutron beams are vetoed by connecting the D1 detector and the A1 and A2 detectors in anticoincidence (in COINC 1). Coincidence channel 3 measures the number of D1 pulses which were vetoed. The D1 pulse and the veto pulse are connected in coincidence; the number of coincidences is a measure of the number of D1 pulses vetoed. Coincidence channel 4 measures the number of D1 events which are accidentally vetoed. The veto pulse is delayed (by inserting DELAY 5) to insure that a valid veto pulse and the associated D1 pulse do not produce a coincidence (in COINC 5); hence, only accidental coincidences between the D1 and veto pulses can occur. The number of D1 events vetoed accidentally are used to correct for the number of real events lost on this account. This correction has been negligible in measurements made thus far.

2-4. Backgrounds

Background events in the time-of-flight spectrum arise from the following sources: (1) accidental or random coincidences, (2) neutron interactions with carbon nuclei in the D1 scintillator, (3) plural scattering of neutrons in the D1 scintillator, and (4) gamma-rays. Each of these backgrounds

and the associated subtraction technique is described in the following subsections.

2-4.1 Accidental Coincidences

If the singles rates in the D1 and D2 detectors are designated N_1 and N_2, respectively, then the number of accidental or chance coincidences A observed per second with a steady beam is given by the well known expression

$$A = N_1 N_2 (\tau_1 + \tau_2) \qquad (3)$$

where τ_1 and τ_2 represent the time durations of the D1 and D2 logic pulses, respectively. Since these uncorrelated D1 and D2 pulses are randomly distributed in time, the resulting background is a level "sea" of events spread over the entire time-of-flight spectrum. With a beam from a pulsed accelerator, the number of accidental coincidences observed per second is given by

$$A = N_1 N_2 (\tau_1 + \tau_2)/f \qquad (4)$$

where f is the duty cycle of the pulsed beam. Since the uncorrelated D1 and D2 signals from the microbeam pulses are not randomly distributed in time, the resulting background may

have a series of peaks with the time interval between the peaks equal to the period between the microbeam pulses; however, if the range of neutron energies in the spectrum is large, the differences in neutron flight-times between the target and the D1 detector may spread out each neutron beam pulse sufficiently to unstructure the spectrum of accidental coincidences.

As described in Section 2-3.2, regions composed only of accidental coincidences are included on both sides of the real events in the time-of-flight spectrum. These regions are used to subtract the background of accidental coincidences when the beam is unstructured; in this case, the level of accidental coincidences is determined by extrapolating the regions of accidental coincidences through the neutron time-of-flight peak. When the accidental-coincidence background is structured, the measured spectrum of accidental coincidences is used to subtract the background from the neutron time-of-flight spectrum.

2-4.2 Carbon Background

Neutron-carbon non-elastic interactions in the D1 scintillator may produce both a detectable charged particle and a secondary neutron. Such interactions are indistinguishable from the desired n-p interactions. Carbon background begins

to become significant above about 15 MeV. At 90 MeV, Kellogg (1953) has shown that all neutron-carbon non-elastic interactions produce charged secondaries, and about 90 percent of these interactions produce secondary neutrons; furthermore, since the total n-C non-elastic cross-section at 90 MeV is approximately 3 times greater than the total n-p cross section, significant carbon background would be expected for high-energy neutrons. At the present time, there is insufficient neutron-carbon cross section data available to compute the carbon background.

A technique has been developed to subtract the carbon background by making separate measurements of the neutron spectrum with Dl scintillators differing in their relative carbon-hydrogen composition. For this purpose, we have used NE-102 plastic scintillator ($CH_{1.105}$) and NE-228 liquid scintillator ($CH_{2.11}$). The ratio of the numerical density of hydrogen in NE-228 to that in NE-102 is 1.26; the carbon ratio is 0.66. This technique assumes that the two time-of-flight spectra have been converted to energy spectra, normalized to the same beam, and corrected for differences in scintil-

lator volume and neutron attenuation. The total number of events R_{2j} in an energy interval j of the NE-228 energy spectrum can be written

$$R_{2j} = R_{2Hj} + R_{2Cj} \tag{5}$$

where the subscript 2 represents NE-228, and R_{2Hj} and R_{2Cj} are the number of events from n-p and n-C interactions, respectively. Likewise, the number of events R_{1j} in the interval j of the NE-102 energy spectrum can be written

$$R_{1j} = R_{1Hj} + R_{1Cj} \tag{6}$$

From the ratios of the numerical densities of hydrogen and carbon in the NE-228 and NE-102 scintillators, we can write

$$R_{2Hj} = 1.26\, R_{1Hj} \tag{7}$$

and

$$R_{2Cj} = 0.66\, R_{1Cj} \tag{8}$$

Substituting these expressions for R_{2Hj} and R_{2Cj} into Eq. (5), we have

$$R_{2j} = 1.26\, R_{1Hj} + 0.66\, R_{1Cj} \tag{9}$$

Solving Eqs. (6) and (9) simultaneously for R_{1Cj} and R_{1Hj},

we find

$$R_{1Cj} = 2.10\, R_{1j} - 1.66\, R_{2j} \tag{10}$$

and

$$R_{1H} = 1.67\, R_{2j} - 1.10\, R_{1j} \tag{11}$$

In a similar manner, the number of n-p and n-C events in the interval j of the NE-228 energy spectrum can be determined as

$$R_{2Cj} = 1.39\, R_{1j} - 1.10\, R_{2j} \tag{12}$$

$$R_{2Hj} = 2.10\, R_{2j} - 1.39\, R_{1j} \tag{13}$$

The number of n-p and n-C events in each interval of the NE-102 and NE-228 energy spectra can be determined from Eqs. (10) through (13).

A requirement of the carbon subtraction technique is that the NE-102 and NE-228 detector thresholds be set at the same level. To energy calibrate these detectors requires a knowledge of the response of both NE-102 and NE-228 to protons. The response of protons in NE-102 can be obtained from the calculated response of Gooding and Pugh (1960, 1961). To obtain the response of NE-228, we measured the response of

NE-228 to 3.5, 5.8, and 10.5 MeV recoil protons from the elastic scattering of 14 MeV protons at the National Research Council, Ottawa, Canada. Madey and Waterman (1972) have described the results of these measurements in a publication written after the period covered by this report.

2-4.3 Plural Scattering Background

A neutron scattered into the D2 detector from a second or higher-order interaction in the D1 scintillator is indistinguishable from a single-scattered neutron. The plural scattering background is expected to be more significant in the lower energy portion of a measured spectrum for two reasons: (1) the neutron mean-free-path for nuclear interactions decreases with decreasing neutron energy, and (2) plural-scattered neutrons which reach the D2 detector generally lose a larger fraction of their incident energy than neutrons scattered once from protons. The significance of the plural scattering background also depends on the shape of the neutron spectrum. On account of the second reason above, the percentage of the background in the low-energy region will be larger in a spectrum in which the number of neutrons increases with energy than in a spectrum in which the number of

neutrons decreases with energy. The magnitude of the background also depends upon the ratio of the diameter of the D1 scintillator to the neutron mean-free-path for nuclear interactions. As this ratio decreases, the probability of plural scattering also decreases. The plural scattering background can be kept at an acceptable level by choosing the dimensions of the D1 scintillator to be smaller than the nuclear interaction mean-free-path for the lowest-energy neutrons in the spectrum.

The information needed to perform a reliable calculation of the plural scattering background would include the differential cross sections of the secondary neutrons from neutron-carbon non-elastic interactions and the light output in the D1 scintillator from the charged particles produced in these interactions. At the present time, there is insufficient cross section data to make a reliable calculation.

The plural scattering background has proved not to be a serious limitation in measurements made thus far with this spectrometer. In measuring the neutron spectrum above 15 MeV at 130 degrees from 740 MeV protons on a thick uranium target, we endeavored to determine the plural scattering back-

ground by measuring the spectrum with Dl scintillators of significantly different diameter. Although the experimental errors were large, this measurement indicated the plural scattering background in this spectrum had an upper limit of about 12 percent; however, because this spectrum decreased steeply with increasing energy, we believe that the plural scattering background is considerably less than 12 percent. In another measurement made with 14 MeV neutrons, the plural scattering background was inferred to be about 15 percent. This measurement is described in Section 2-8.1. It is interesting to note that in this measurement the plural-scattered neutrons were separated from the real events by time-of-flight.

2-4.4 Gamma-Rays

Since gamma-rays are separated from neutrons by time-of-flight, a low gamma-ray background does not present a problem. With the exception of a preliminary measurement of neutrons in the 1 to 30 MeV region at the University of Rochester, gamma-rays have not been a problem in measurements made thus far and additional gamma-ray discrimination has not been needed.

In the measurement at the University of Rochester, an intense gamma-ray background increased the singles rates in the detectors and resulted in a high rate of accidental coincidences. Although a useable ratio of real to accidental coincidences was achieved by reducing the beam intensity, the resulting count rate was a rather low 5 counts per minute. The high singles rates in the individual detectors of the spectrometer precluded the use of conventional pulse-shape-discrimination (PSD) systems to discriminate against gamma-rays. Since conventional PSD systems analyze each event in the detector, blocking losses occur at high singles rates. Such blocking losses were encountered by Osborn and Madey (1969a) in an early measurement of 14 MeV neutrons with a conventional PSD system.

To improve the performance of the spectrometer in applications involving very high gamma-ray backgrounds, Baldwin (1971) undertook as a Masters thesis problem the development of a gated PSD system for high data aquisition rates. This system employs a linear gate between the photomultiplier anode signal and the appropriate pulse-shape-discrimination circuitry. The linear gate is triggered by the

occurence of a coincidence between events in the D1 and D2 detectors (COINC 2 in Fig. 4). By looking at only those signals from the D1 detector that occur in coincidence with a D2 signal, the number of D1 signals that are analyzed by the PSD system is greatly reduced.

For pulse-shape-discrimination, we use NE-213 liquid scintillator. In order to subtract background from neutron-carbon interactions, a second PSD scintillator is needed which has a significantly different carbon-hydrogen composition. We have not searched for such a scintillator because gamma-rays have not been a problem in measurements made thus far.

2-5. Performance Characteristics

2-5.1 Energy Resolution

The relative uncertainty $\Delta T'/T'$ in the measurement of the scattered neutron kinetic energy, which can be derived from Eq. (1), is

$$\Delta T'/T' = \frac{(T' + M)\ (T' + 2M)}{M^2} \left[\left(\frac{\Delta X}{X}\right)^2 + \left(\frac{t}{t}\right)^2 \right]^{\frac{1}{2}} \qquad (14)$$

where ΔX is the uncertainty in the neutron flight path and Δt is the intrinsic time dispersion of the system. The relative uncertainty $\Delta T/T$ in the incident neutron kinetic energy, which

can be derived from Eq. (2), is

$$\Delta T/T = \frac{2M\cos\theta}{[(T' + 2M)\cos^2\theta\,] - T'} \left[\left(\frac{\Delta T' \cos\theta}{T'} \right)^2 + (2\,\Delta\theta\,\sin\theta)^2 \right]^{\frac{1}{2}} \quad (15)$$

where $\Delta\theta$ is the uncertainty in the neutron scattering angle.

The uncertainty ΔX in the neutron flight path and the uncertainty $\Delta\theta$ in the neutron scattering angle are both a result of the finite dimensions of the D1 and D2 scintillators. Waterman (1973) has written computer programs (in FORTRAN IV) to compile histograms of the distributions of flight-paths and scattering angles for neutrons scattered from the D1 scintillator into the D2 scintillator. Each of these uncertainties are taken to be the half-width at half-maximum of the distribution. The intrinsic time dispersion Δt of the system is minimized by using constant-fraction of pulse-height timing discriminators for the D1 and D2 detectors. In Figure 5, the time dispersion with the $2\frac{1}{2}$ inch diameter by $2\frac{1}{2}$ inch high D1 detector and the 9 inch diameter by 8 inch thick D2 detector is 2.2 nanoseconds (fwhm) for a dynamic range of pulse-heights of 10 to 1 from a cobalt-60 source.

For the two detectors mentioned in the above paragraph, the energy resolution is shown in Fig. 6 for neutron

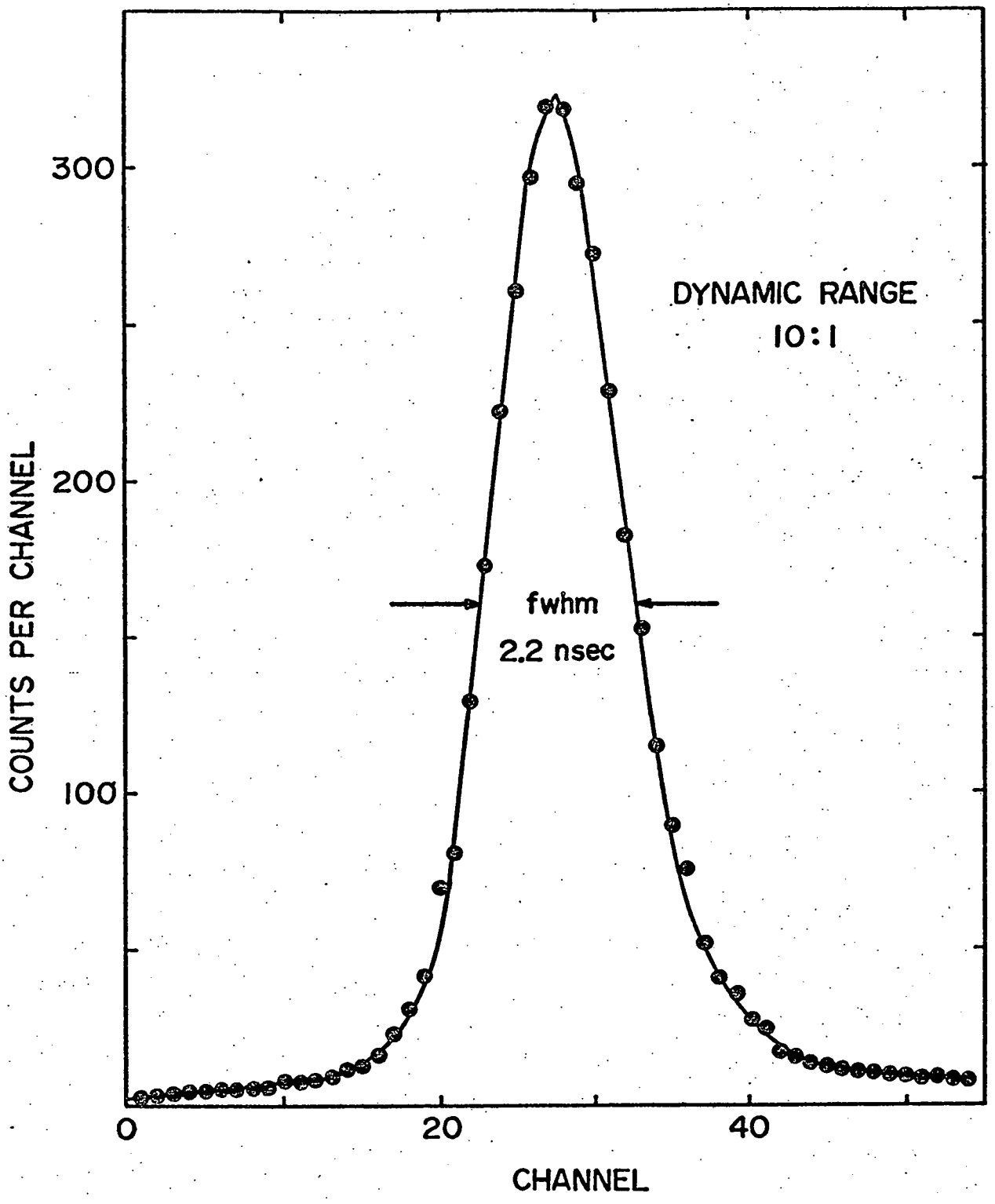

FIG. 5 The time resolution obtained with a $2\frac{1}{2}$ inch diameter by $2\frac{1}{2}$ inch high D1 scintillator and a 9 inch diameter by 8 inch thick D2 scintillator for a dynamic range of pulse-heights of 10:1 from a cobalt-60 source. The intrinsic time dispersion is 2.2 nsec (fwhm).

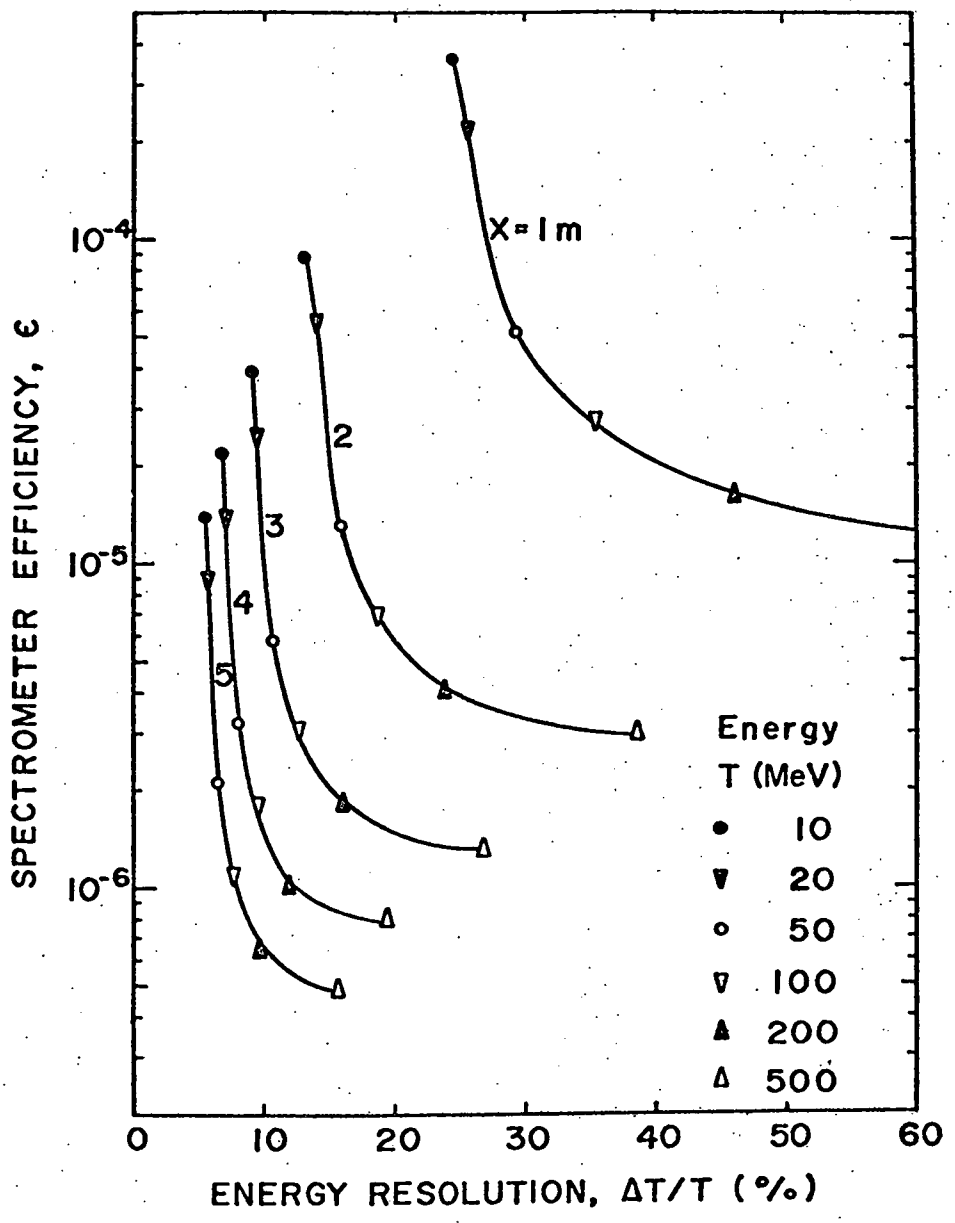

FIG. 6 The efficiency and energy resolution for neutron energies from 10 to 500 MeV and neutron flight paths of from 1 to 5 meters for a spectrometer consisting of a $2\frac{1}{2}$ inch diameter by $2\frac{1}{2}$ inch high NE-228 D1 scintillator and a 9 inch diameter by 8 inch thick NE-102 D2 scintillator positioned at an angle of 40 degrees with respect to the direction of the incident neutrons at the D1 scintillator. A distance of 15 meters was assumed between the target and D1 scintillator.

energies from 10 to 500 MeV and for flight-paths from 1 to 5 meters; for example, for a mean-flight path of 4 meters, the energy resolution varies from 7 percent at 10 MeV, to 9 percent at 100 MeV, to 20 percent at 500 MeV.

2-5.2 Spectrometer Efficiency

For neutrons with kinetic energy T, the spectrometer efficiency is defined as the ratio of the number of neutrons/sec detected to the number of neutrons/sec incident on the spectrometer. The expression for the spectrometer efficiency as a function of the incident neutron energy and the neutron scattering angle is derived in the following paragraphs.

The differential probability $dP\ (T,\vec{\Omega}_1,\vec{\Omega},x,y,z)$ per unit time that a neutron with kinetic energy T in a differential kinetic energy interval dT will scatter elastically from a proton in a volume element dV of the D1 detector and escape in a direction $\vec{\Omega}$ within a differential solid angle $d\Omega$ is given by

$$dP\ (T,\vec{\Omega}_1,\vec{\Omega},x,y,z) = f(T,\vec{\Omega}_1)\ dT\ d\Omega_1 n_H g_1(T,x,y,z)$$

$$\cdot \sigma(T,\vec{\Omega}) g_2(T,\vec{\Omega},x,y,z)\ d\Omega\ dL \qquad (16)$$

Here $\vec{\Omega}_1$ is the incident neutron direction measured with respect to the direction of the beam that produces the neutrons; $f(T,\vec{\Omega}_1)dTd\Omega_1$

is the number of neutrons produced at a source per unit time within a differential kinetic energy interval dT about the energy T and within a differential solid angle interval $d\Omega_1$ about the direction $\vec{\Omega}_1$; the solid angle interval $d\Omega_1$ represents the solid angle subtended by a differential volume element dV of the D1 detector at the neutron source; n_H is the numerical density of hydrogen in the D1 detector; $g_1(T, x, y, z)$ is the attenuation of the incident neutrons in reaching the volume element dV centered at the coordinates x, y, z; $\sigma(T,\vec{\Omega})$ is the cross-section per proton for elastically scattering a neutron with kinetic energy T in a direction $\vec{\Omega}$ measured with respect to the incident neutron direction $\vec{\Omega}_1$; $g_2(T,\Omega,x,y,z)$ is the attenuation of neutrons scattered in the direction $\vec{\Omega}$ from the volume element dV of the D1 detector; and dL is the path-length through the volume element dV in the direction parallel to $\vec{\Omega}_1$.

In practice, the D1 detector is positioned at a distance from the neutron source which is large compared with the dimensions of either the D1 detector or the neutron source. Although this spacing is usually

defined by the shielding material and neutron collimator between the D1 detector and neutron source, it is important that this distance be large so that the uncertainty in the direction of neutrons incident on the D1 detector is small. Since the neutron scattering angle is measured with respect to the incident neutron direction, the direction of the incident neutrons must be well defined in order to reduce the uncertainty in the neutron scattering angle. If the distance between the source and the D1 detector is large compared with the dimensions of the source and D1 detector, the solid angle $d\Omega_1$ subtended by each volume element of the D1 detector is given to a good approximation by

$$d\Omega_1 = dA/X1^2 \tag{17}$$

where dA is the cross-sectional area of the volume element dV normal to the direction $\vec{\Omega}_1$. Furthermore, since the divergence of the initial beam is small, the cross-sectional area dA is approximately equal to dy dz, the cross-sectional area of the volume element dV. Also, since the divergence of the incident beam is so small, the path length dL through the volume element parallel to incident neutron direction $\vec{\Omega}_1$ can be represented by dx. Also in this approxi-

mation of a nearly parallel neutron beam, the quantity $f(T,\vec{\Omega}_1)$ can be regarded to be independent of the production direction $\vec{\Omega}_1$ over the dimensions of the D1 detector. Substituting Eq. (17) and noting that $dV = dxdA$, we can rewrite Eq. (16) as

$$dP\ (T,\vec{\Omega}_1,\ \vec{\Omega},x,y,x) = f(T,\vec{\Omega}_1)dT\ n_H\ g_1(T,x,y,z)\ \sigma\ (T,\ \vec{\Omega})$$

$$\cdot\ g_2(T,\vec{\Omega},x,y,z)\ d\Omega dV/X1^2 \qquad (18)$$

The expression for the differential counting rate $dR(T,\ \vec{\Omega}_1,\vec{\Omega}\ )$ of neutrons with kinetic energy T within a differential kinetic energy interval dT can be written as

$$dR(T,\vec{\Omega}_1,\vec{\Omega}) = \varepsilon_2(T,\vec{\Omega}) \int_V \int_\Omega dP(T,\Omega_1,\Omega,x,y,z) \qquad (19)$$

where $\varepsilon_2(T,\vec{\Omega})$ is the probability or efficiency for detecting neutrons scattered in the direction $\vec{\Omega}$ in the D2 detector. The double integration is carried out over the volume V of the D1 detector and over the solid angle Ω subtended by the D2 detector at the volume element dV. In practice, the distance between the D1 and D2 detectors is chosen to be large so that the neutron flight-path is large compared with the uncertainty in the flight-path. In this case, the solid angle Ω subtended by the D2 detector at each

volume element of the D1 detector is approximately equal to the solid angle Ω_2 subtended by the D2 detector at the center of the D1 detector. Furthermore, the differential cross-section $\sigma(T,\Omega)$ can be considered independent of the direction $\vec{\Omega}$ of the scattered neutron over the dimensions of the D2 detector. In this approximation, integration of Eq. (19) over the solid angle Ω can be written as

$$\int_{\Omega} \sigma\ (T,\vec{\Omega})\ d\Omega = \sigma\ (T,\vec{\Omega})\ \Omega_2 \qquad (20)$$

Integration of Eq. (19) over the volume is evaluated numerically by a computer subroutine called ATTN written by Waterman (1973). The result of the integration of the attenuation factors g_1 and g_2 over the volume of the D1 detector yields an effective volume $V'(T,\vec{\Omega})$ which is a function of the neutron energy. Integration over the volume can be expressed as

$$\int_{V} g_1(T,x,y,z)g_2(T,\vec{\Omega},x,y,z)dV = V'\ (T,\vec{\Omega}) \qquad (21)$$

The effective volume $V'(T,\vec{\Omega})$ is a fraction $G(T,\vec{\Omega})$ of the actual volume

$$G(T,\vec{\Omega}) \equiv V'(T,\vec{\Omega})/V \qquad (22)$$

where $G(T,\Omega)$ is defined as the total attenuation factor. Substituting Eqs. (20), (21), and (22) into Eq. (19), the differential counting rate can be expressed as

$$dR(T,\vec{\Omega}_1,\vec{\Omega}) = \varepsilon_2(T,\vec{\Omega})\ f(T,\vec{\Omega}\ )\ n_H G(T,\vec{\Omega})\sigma\ (T,\vec{\Omega})\Omega_2 V\ dT/X1^2 \qquad (23)$$

The differential number $dN_o(T,\vec{\Omega}_1)$ of neutrons/sec incident on the spectrometer within a differential kinetic energy interval dT about the energy T is given by

$$dN_o\ (T,\vec{\Omega}\ ) = dT \int_{\Omega_1} f(T,\vec{\Omega}_1)\ d\Omega_1 \qquad (24)$$

where the integration of the solid angle Ω_1 is carried out over the dimensions of the D1 detector. Integration of Eq. (24) gives

$$dN_o(T,\vec{\Omega}_1) = f(T,\vec{\Omega}_1)\ \Omega_1 dT \qquad (25)$$

where $\vec{\Omega}_1$ is the solid angle subtended by the D1 detector at the neutron source.

The spectrometer efficiency $\varepsilon(T,\Omega)$ is given by the ratio of $\frac{dR}{dT}$ from Eq. (23) to $\frac{dN_o}{dT}$ from Eq. (25):

$$\varepsilon(T,\vec{\Omega}) = \frac{\varepsilon_2(T,\vec{\Omega})\, n_H G(T)\, \sigma\,(T,\vec{\Omega})\Omega_2 V}{X1^2 \Omega_1} \qquad (26)$$

Since n-p elastic scattering has azimuthal symmetry about the direction of the incident neutron, Eq. (26) can be written in terms of the neutron scattering angle θ as

$$\varepsilon(T,\theta) = \frac{\varepsilon_2(T,\theta) n_H G(T) \sigma(T,\theta)\Omega_2 V}{X1^2 \Omega_1} \qquad (27)$$

The spectrometer efficiency is plotted in Fig. 6 versus the energy resolution for neutron energies from 10 to 500 MeV and for neutron flight-paths from 1 to 5 meters. These values were computed from Eq. (27) for a spectrometer configuration consisting of a $2\frac{1}{2}$ inch diameter by $2\frac{1}{2}$ inch high NE-228 D1 detector and a 9 inch diameter by 8 inch thick D2 detector and for a neutron scattering angle of 40 degrees. A distance of 15 meters was assumed between the target and the D1 detector. Figure 6 permits the overall performance of the spectrometer to be evaluated as a function of the neutron energy and flight-path. The configuration for any particular measurement generally represents a compromise between

count rate and energy resolution.

2-5.3 Count-Rate Capability

In practice, the count-rate capability of the spectrometer is limited by the rate of accidental coincidences rather than by blocking losses. As the beam intensity is raised, the rate of real coincidences increases linearly with the beam intensity, whereas the rate of accidental coincidences increases as the square of the beam intensity. When the ratio of real to accidental coincidences becomes much less than 1, a small error in the determination of the number of accidental coincidences results in a significant error in the number of real events. The rate of accidental coincidences can be reduced by shielding the D2 detector from the target and from stray radiation to reduce the event rate in this detector.

Blocking studies conducted with 14 MeV neutrons showed that the multichannel analyzer,† which is the slowest unit in the electronic configuration, could accept count rates of 300 counts/sec with 1 percent blocking. The blocking level of the D1 detector was not reached at a singles rate of 10^6 counts/sec, which was the maximum rate attainable with the beam. Blocking has not occurred (in either the detectors or the analyzer) in

† Northern Scientific Model NS-605

measurements made thus far because the count rates of real events were limited to about 1 count/sec by accidental count rates of the same order of magnitude.

It should be noted that real events may be "blocked" by accidental coincidences if the rate of accidental coincidences is large in comparison to the rate of real events. Whenever a scattered neutron from a real event is detected in the D2 detector, the coincidence (COINC 2 in Fig. 4) is "open" for a time interval equal to the duration τ_2 of the D2 logic pulse (typically 250 nsec). The probability P_1 that an uncorrelated D1 pulse from a random event will arrive at the coincidence module during this time interval τ_2 is

$$P_1 = N_1 \tau_2 / f \qquad (28)$$

where N_1 is the observed singles rate in the D1 detector and f is the duty cycle of the beam. In practice, the timing of the electronics is adjusted to record the real events in the central portion of the time-of-flight spectrum with regions of accidental coincidences on either side; therefore, for real events, the wide D2 pulse precedes the narrow D1 pulse to the coincidence module (COINC 2 in Fig. 4) by about $\tau_2/2$ nsec.

It is only during this interval $\tau_2/2$ that the valid D1 pulse can be "blocked" by a random D1 pulse; hence, the probability P_2 that a real event will be "blocked" or lost is

$$P_2 = N_1\tau_2/2f \tag{29}$$

In measurements made thus far, less than 2 percent of the real events have been lost on this account.

2-6. Typical Time-of-Flight Spectra

Typical neutron time-of-flight spectra are plotted in Figs. 7 (a) and 8 (a). The spectra shown in Fig. 7 were generated by neutrons from about 50 to 400 MeV produced by stripping 447 MeV deuterons on a 3/8-inch beryllium target. The spectra shown in Fig. 8 were generated by neutrons from 15 to about 140 MeV produced at 130 degrees by 740 MeV proton bombardment of a thick uranium target.

In Figs. 7 (a) and 8 (a), the narrow peak on the left is the gamma-ray time-of-flight peak; the broad central peak is the neutron time-of-flight peak; and the spike at the right edge is an instrumental artifact caused by accidental coincidences in which the TAC start and stop signals were both

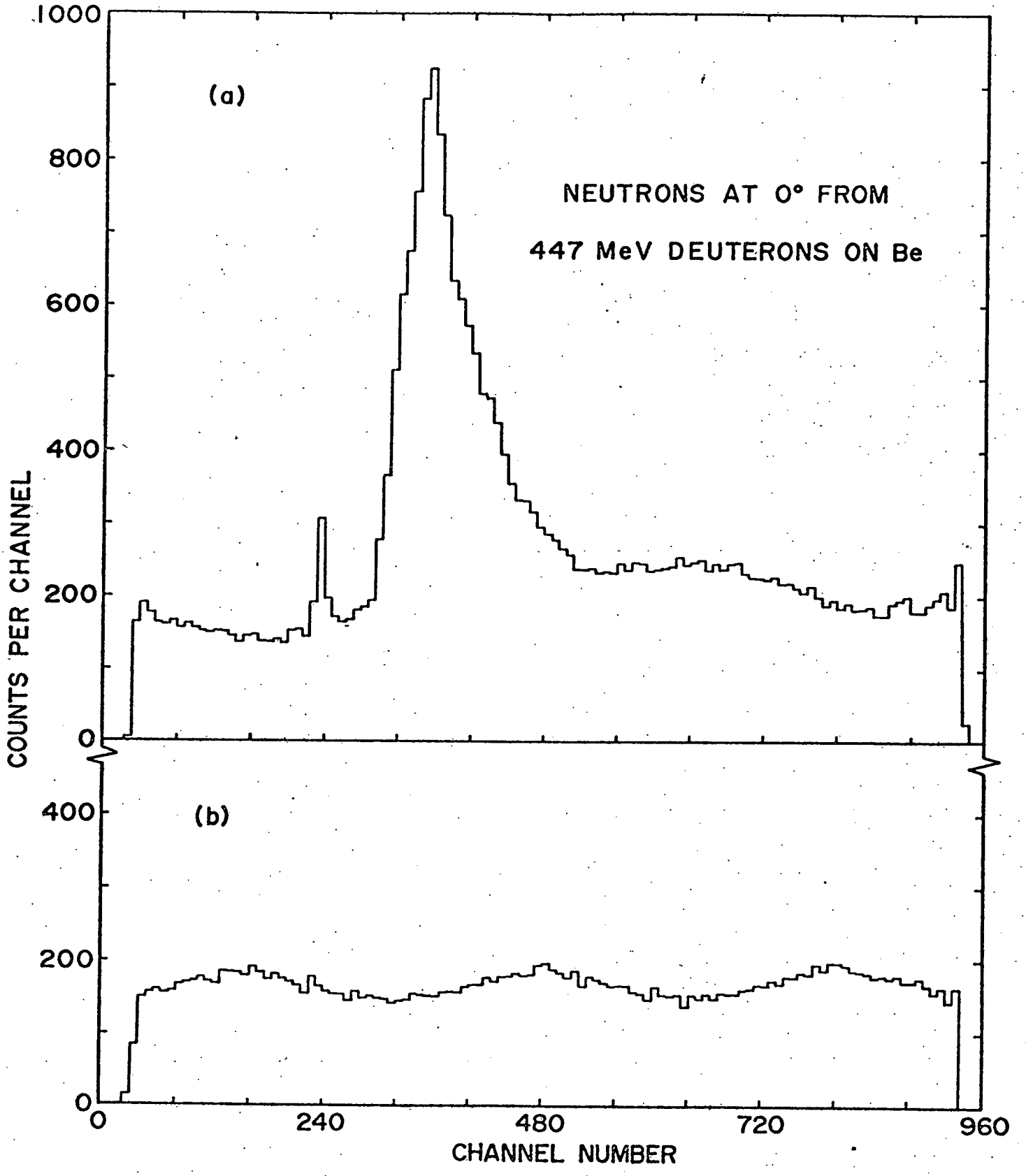

FIG. 7 (a) Neutron time-of-flight spectrum and (b) spectrum of accidental coincidences at 0 degrees from 447 MeV deuterons on a 3/8-inch thick beryllium target.

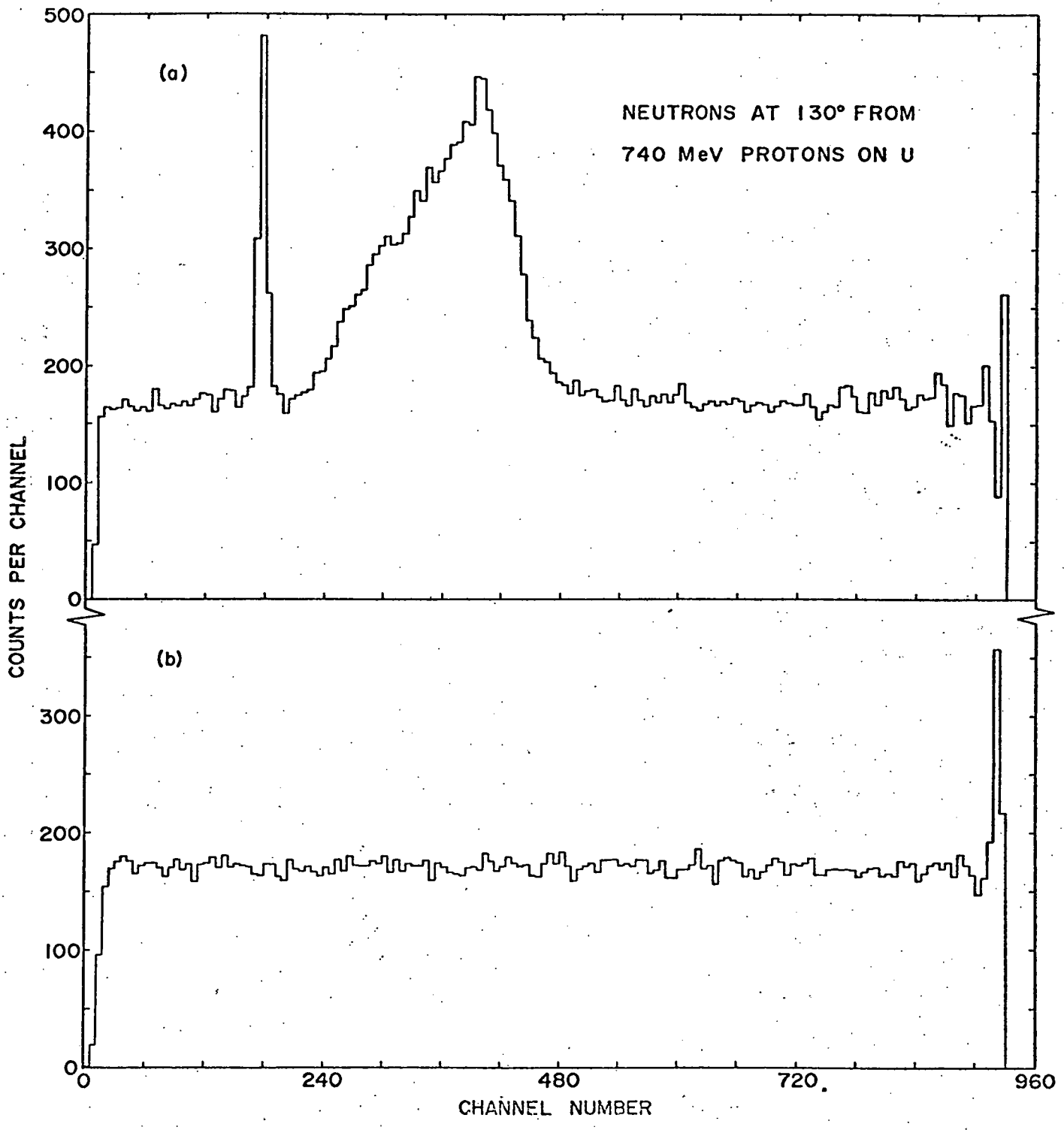

FIG. 8 (a) Neutron time-of-flight spectrum and (b) spectrum of accidental coincidences at 130 degrees from 740 MeV protons on a 30-cm thick uranium target.

timed on the D2 detector pulse. The regions to the left and right of the time-of-flight peaks are composed entirely of accidental coincidences. The accidental-coincidence spectrum in Fig. 7(b) has a period structure of the accidentals in Fig. 7(b) is out of phase with the periodic structure; whereas that in Fig. 8(b) is unstructured. The periodic structure of the accidentals in Fig. 7(b) is out of phase with the periodic structure of the accidentals in Fig. 7(a) because these spectra were measured with different coincidence circuits.

2-7. Analysis of a Time-of-Flight Spectrum

The first step in the analysis of a time-of-flight spectrum is to subtract the background of accidental coincidences in the manner described in Section 2-4.1. The time-of-flight spectrum can then be converted to an energy spectrum by computing the incident neutron energy T_i corresponding to each channel i of the time-of-flight spectrum. To determine the incident neutron energy T_i, it is first necessary to determine the time-of-flight t_i corresponding to each channel i of the spectrum. The flight-time t_i is determined from the mean channel of gamma-ray time-of-flight peak and the time calibration of the analyzer. If channel g denotes the mean channel of the gamma-ray peak, the time-of-flight corresponding to channel g is given to a good approximation by

$$t_g = X/c \tag{30}$$

where X is the gamma-ray flight path defined as the distance between the centers of the D1 and D2 detectors, and c is the speed of light. The time difference Δt_{gi} between any channel i in the spectrum and channel g is given by

$$\Delta t_{gi} = (g-i)T_c \tag{31}$$

where T_c is the time calibration of the analyzer expressed in units of nanoseconds per channel. The time-of-flight t_i corresponding to any channel of the spectrum is then

$$t_i = X/c + (g - i)\, T_c \tag{32}$$

From Eq. (1), the scattered neutron kinetic energy T_i' corresponding to channel i is given by

$$T_i' = M\,[1/(1-X^2/c^2t_i^2)^{\frac{1}{2}} - 1] \tag{33}$$

From Eq. (2), the incident neutron kinetic energy T_i corresponding to channel i is given by

$$T_i = 2M/\,[(1+2M/T_i')\cos^2\theta - 1] \tag{34}$$

To improve the statistics, several channels can be combined into energy intervals of approximately the same energy

width; alternatively, the size of the intervals can be chosen to correspond to the energy resolution of the spectrometer. It should be noted that the energy interval represented by each channel is nonuniform; therefore, it is not possible to regroup the data in intervals of precisely the same energy width.

For neutron spectra above 15 MeV, the carbon background must be subtracted as described in Section 2-4.2. The spectrometer efficiency as given by Eq. (27) is a function of the neutron energy; therefore, a correction must be made to each energy interval of the measured spectrum for differences in the spectrometer efficiency. The correct relative energy spectrum is obtained by dividing the number of events per MeV observed in each energy interval by the corresponding spectrometer efficience $\varepsilon(T)$.

2-8. Performance of the Spectrometer with Monoenergetic Neutrons

The performance of the spectrometer has been studied at both 14 and 220 MeV with monoenergetic neutrons. The results of these measurements are given in the following subsections.

2-8.1 Performance at 14 MeV

The performance of the spectrometer at 14 MeV was

studied from the results of several experiments conducted at the National Research Council, Ottawa, Canada. There were two distinct advantages in these experiments with 14 MeV neutrons:

(1) The neutrons are monoenergetic. The spread in the neutron energy is negligible in comparison with the energy resolution of the spectrometer.

(2) At the National Research Council at Ottawa, the absolute intensity of the 14 MeV neutrons can be monitored with a precision long counter calibrated with the Canadian National Standard americium-beryllium source. The knowledge of the absolute neutron intensity permits comparison of the calculated and observed count rates.

In July and December of 1968, Osborn and Madey (1969a, b) confirmed the principle of the spectrometer; but the count rate was found to be limited by blocking in the time-to-amplitude converter (TAC) unit. At the National Research Council in January 1970, Waterman et al. (1970) tested an electronic scheme which eliminated the TAC blocking. During these measurements, deficiencies were found in the technique then used to calibrate the discriminator bias levels. This technique was based on the

extrapolated upper edge of the sodium-22 Compton spectrum as defined by Verbinski (1968). In June and November, 1970, we tested a technique for energy calibration of the detectors using the peaks of the Compton spectra as calibration points. During the November, 1970 measurements, we compared the performance of constant-fraction-timing discriminators to the performance of leading-edge discriminators. Also during the November 1970 run, Madey and Waterman (1973) measured the response of NE-228 liquid scintillator to 3.5, 5.8, and 10.5 MeV recoil protons from elastic scattering of 14 MeV neutrons.

In the remainder of this section, the results of a time-of-flight measurement made in November 1970 will be described as an example of the spectrometer performance at 14 MeV. In this measurement, 14 MeV neutrons produced by the t(d, n) α reaction were incident on a $2\frac{1}{2}$ inch diameter by $2\frac{1}{2}$ inch high NE-228 D1 scintillator which was positioned 70 cm from the target and at an angle of 98 degrees with respect to the incident deuteron beam. The D2 detector, which consisted of a 4 inch diameter by 4 inch thick NE-102 plastic scintillator, was positioned 175 cm from the D1 detector and at an angle of 40 degrees with respect

to the direction of the incident neutrons at the D1 detector.

The measured energy spectrum is plotted as a histogram in Fig. 9. The region of the spectrum above 11.3 MeV was normalized to a Gaussian distribution which was required to have a half-width at half-maximum equal to the computed energy resolution (of 11 percent). This Gaussian distribution is shown as a dashed curve in Fig. 9. Comparison of this Gaussian distribution with the measured spectrum indicates that the observed and computed energy resolutions agree.

The measurement shown in Fig. 9 was made using constant-fraction-timing discriminators. In a separate measurement, we compared the resolution of the spectrometer with constant-fraction-timing discriminators to that with leading-edge discriminators. The time resolution with the constant-fraction-timing discriminators was significantly better; the fwhm of the 14 MeV neutron peak was 5.3 nsec with the leading-edge discriminators and 3.8 nsec with the constant-fraction-timing discriminators. The corresponding energy resolution is 14 percent with the leading-edge discriminators and 11 percent with the constant-fraction-timing discriminators. Note that the fwhm of the 14 MeV neutron

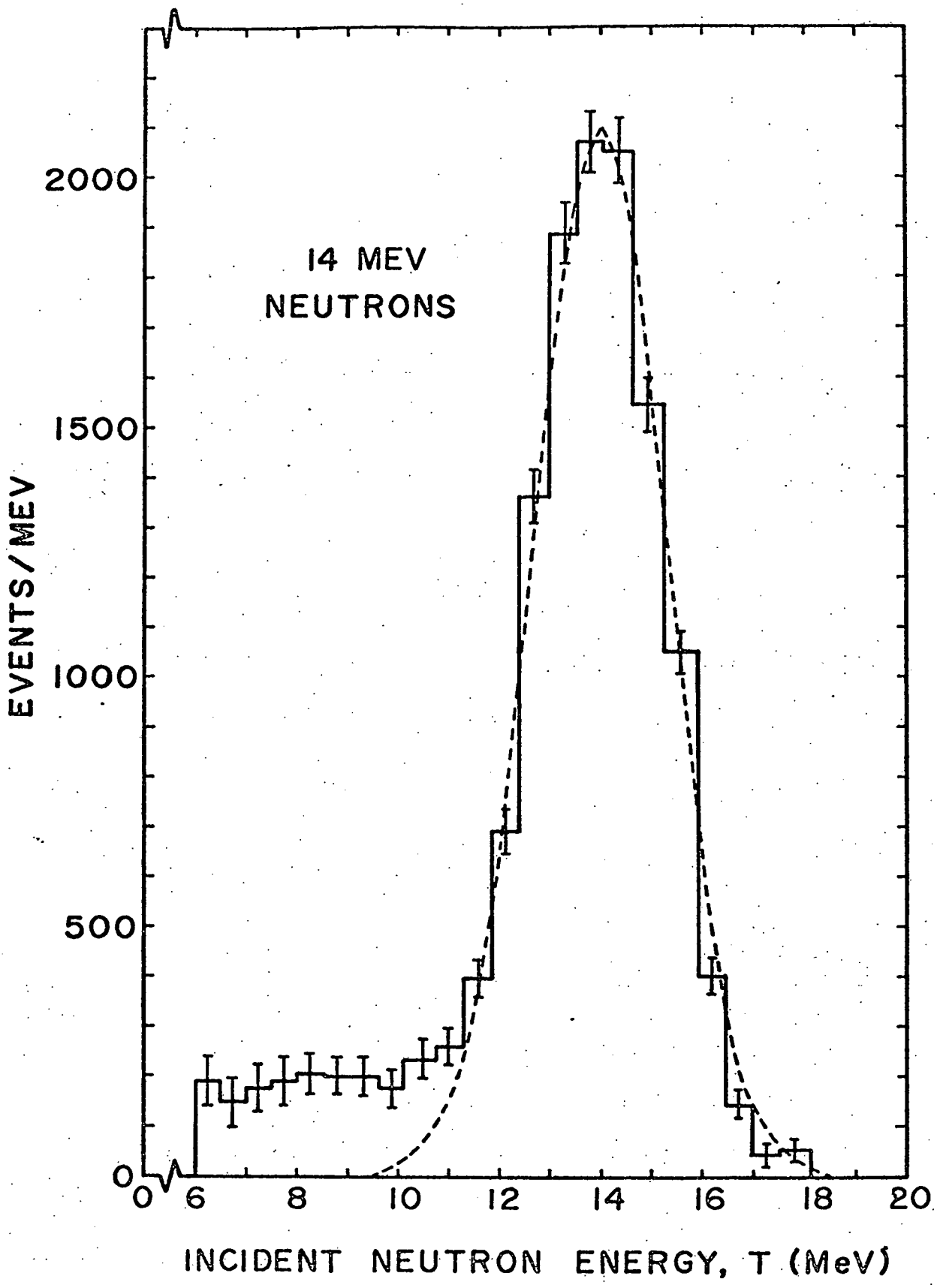

FIG. 9 Measured spectrum of 14 MeV neutrons. The region of the spectrum above 11.3 MeV was normalized to a Gaussian distribution (shown as a dashed curve) required to have a half-width at half-maximum equal to the computed energy resolution of the spectrometer.

peak is greater than that shown in Fig. 5 for gamma-rays. The 14 MeV neutron peak has a fwhm of 3.8 nsec whereas the gamma-ray peak has a fwhm of 2.2 nsec. This difference arises because the scattered neutrons have a distribution of energies and velocities corresponding to the uncertainty $\Delta\Theta$ in the neutron scattering angle Θ. Gamma-rays, on the other hand, travel at the speed of light regardless of energy.

A precision long counter (PLC) similar in design to that first built by Hanson and McKibben (1947) was used to measure the neutron flux produced at the target. This knowledge of the neutron source strength permitted the observed and calculated count rates to be compared. For this measurement, we expected about 7000 events and obtained 6850 events within the Gaussian distribution shown in Fig. 9. If the number of events in the Gaussian distribution is taken to be the true number of real events, then the computed and observed count rates agree to within about 2 percent. The plateau of events in the low-energy region from 6 to 11 MeV is attributed to plural scattering background. A total of 7950 events were observed in the time-of-flight spectrum. This indicates that the plural scattering background comprised

approximately 15 percent of the total number of events in the time-of-flight spectrum.

The energy resolution of the spectrometer at 14 MeV is potentially much better than 11 percent. The D1 detector was positioned 70 cm from the target to enhance the count rate; however, this increased the uncertainty $\Delta\theta$ in the neutron scattering angle. If the D1 detector had been positioned further from the target, the resolution would have been improved. As indicated in Fig. 4, an energy resolution of 6 percent is attainable at 14 MeV with a 4 meter flight-path.

2-8.2 Performance at 220 MeV.

Although there are no truly monenergetic high-energy neutron beams, an approximately monoenergetic neutron beam can be produced by the deuteron stripping process. The performance of the spectrometer at approximately 220 MeV was studied by measuring the neutrons produced at zero degrees by stripping 447 MeV deuterons with a 3/8-inch thick beryllium target at the Lawrence Berkeley Laboratory. For 447 MeV deuterons, the stripping theory of Serber (1947a) predicts a mean neutron energy of 223.5 MeV with an energy spread of approximately 47 MeV (fwhm).

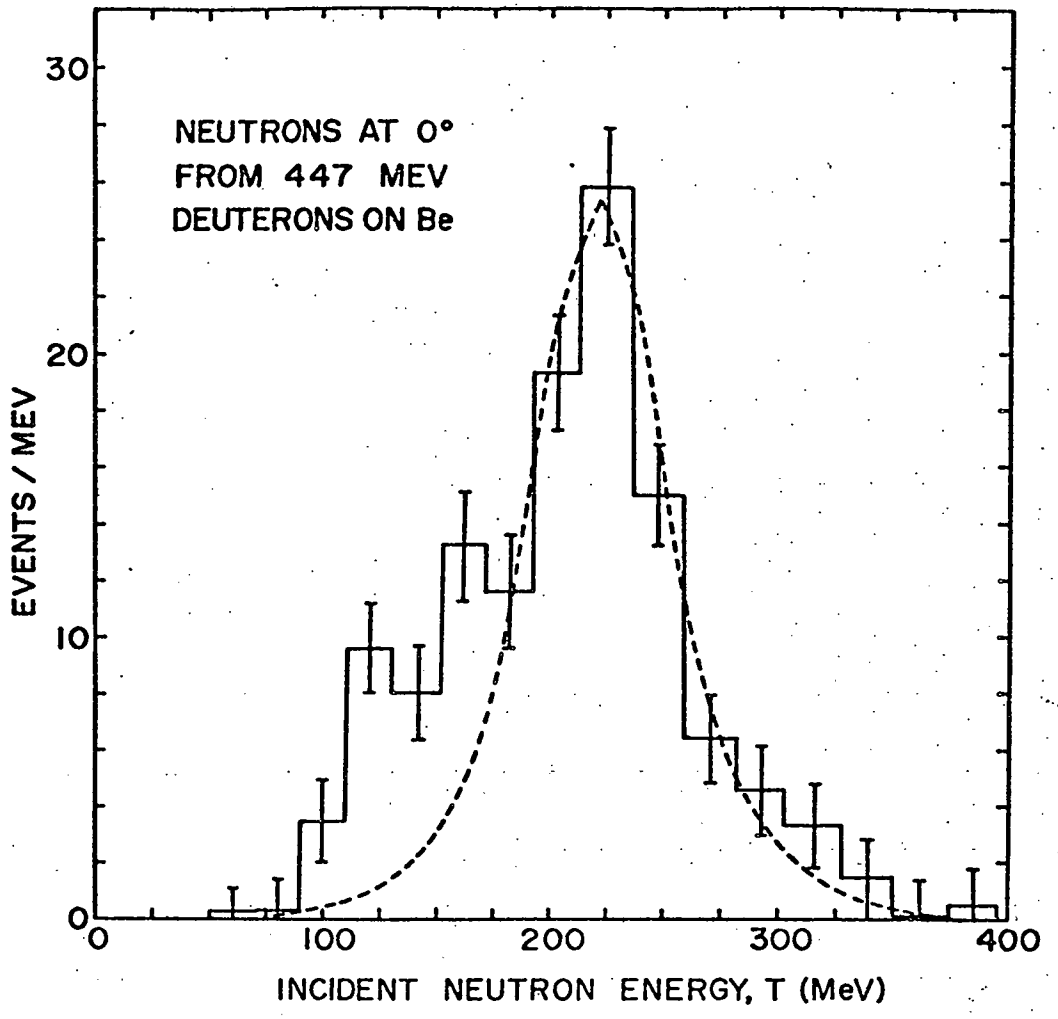

FIG. 10 Measured spectrum of neutrons at 0 degrees from 447 MeV deuterons on a 3/8-inch beryllium target. The resolution broadened spectrum predicted by the Serber stripping theory is shown as a dashed curve.

The large A1, A2, D1, and D2 scintillators described in Section 2-3.1 were used for this measurement. The neutron beam was viewed at approximately 15 meters from the target through a rectangular aperture 2 inch wide by 2 inch high in a 4 foot long steel collimator, which was embedded in the concrete wall shielding the cyclotron. The D2 detector was positioned 5 meters from the D1 detector and at an angle of 50 degrees with respect to the direction of the incident neutrons at the D1 detector. Separate measurements were made with NE-102 plastic and NE-228 liquid D1 scintillators to permit subtraction of the carbon background. The NE-228 spectrum is shown in Fig. 7. The carbon background in the time-of-flight spectra was extensive. The carbon background comprised 85 percent of the real events in the spectrum measured with the NE-102 D1 scintillator and 74 percent in the spectrum measured with the NE-228 D1 scintillator.

The measured energy spectrum is plotted as a histogram in Fig. 10. The computed energy resolution at 220 MeV is 10 percent. The resolution-broadened theoretical spectrum, which was normalized to the region of the observed spectrum above 175 MeV, is shown as a dashed curve. The agreement between the fwhm of the observed and theoretical spectra indi-

cates that the computed energy resolution is correct. The events above the theoretical curve in the region from 100 to 175 MeV are attributed to direct interactions of the deuterons with the beryllium nucleus. An abundance of low-energy neutrons was also observed by Hadley et al. (1949) in the neutron spectrum produced by stripping 190 MeV deuterons on a 1.27 cm thick beryllium target. Since an absolute neutron monitor was not available for this measurement, we could not verify the spectrometer efficiency.

3. MEASUREMENT OF THE NEUTRON SPECTRA FROM 740 MeV PROTONS ON A THICK URANIUM TARGET

3-1. Introduction

The purpose of Section 3 is to describe the measurement of the neutron spectra from 740 MeV protons on a 30-cm thick depleted uranium target at the Lawrence Berkeley Laboratory (LBL). Three separate measurements are reported: from 20 to 500 MeV at 50 degrees; from 1 to 15 MeV at 130 degrees; and from 15 to 140 MeV at 30 degrees with respect to the proton beam. The 50 degree measurements were made in January 1971; the 130 degree measurements in March 1971.

The general purpose of these measurements was to test the degree of validity of the Monte Carlo calculation based on the intranuclear cascade model. Bertini (1963,1965,1967,1969) has compared the predictions of the intranuclear cascade model to thin target measurements in the energy region from 30 to 2900 MeV. Although these comparisons show that the intranuclear cascade model gives a good description of many nuclear reactions involving nucleons on complex nuclei, they also point out the existence of a number of discrepancies. Similarly, discrepancies exist between thick-target measure-

ments and theory. Comparisons of thick target measurements and theory have been reported by Fullwood et al. (1972), Wachter et al. (1967, 1972), Alsmiller (1969). Fullwood et al (1972) have carried out Monte Carlo calculations of the neutron production from medium-energy proton bombardment of heavy-metal targets. The purpose of these calculations was two-fold: (1) to predict the amount of shielding required by the Los Alamos Meson Physics Facility (LAMPF), and (2) to develop a high-intensity pulsed neutron source generated by 800 MeV protons from the LAMPF accelerator. To test the validity of these calculations, Los Alamos (LASL) set up an experiment at the Lawrence Berkeley Laboratory (LBL) 184-inch cyclotron to measure the neutron spectra from 740 MeV protron bombardment of a 30-cm thick depleted-uranium target. We were invited to participate in these measurements and, in particular, to measure the high-energy or cascade region of the spectrum. In a companion experiment with different techniques, Veeser et al. (1972, 1973) measured the evaporation neutron spectra from 60 keV to 10 MeV at both 50 and 130 degrees.

Prior to these measurements, the data of Fraser, Hewitt, and Walker (1966) represented the only measurements available on neutron spectra from heavy-metal targets at proton bombarding energies above the pion production threshold. Fraser et al. measured the neutron spectra produced at angles of 45, 90, and 135 degrees by 1 GeV protons on a lead target 20 cm diameter by 30 cm thick. Fullwood et al. (1972) have calculated the neutron production from 800 MeV protons on a lead target 15 cm diameter by 30 cm thick and compared these calculations with the data of Fraser et al. At 10 MeV, the experimental results are 20 to 40 percent higher than the calculated values. From 30 to 150 MeV, the agreement is good for the 45 degree spectrum, fair at 90 degrees, and poor at 135 degrees. At each angle, the measured yield is higher than the calculated yield.

3-2. Experimental Arrangement

Figure 11 is a simplified diagram of the experimental arrangement. The target consisted of twelve 15 cm diameter by 2.5 cm thick disks of depleted uranium-238 held together by a 3mm thick steel casing. The 740 MeV proton beam from the 184-inch cyclotron traveled through air and struck the 30 cm thick target on axis. The beam spot for the measurement at 50 degrees was approximately 4 cm high by 7 cm wide; at 130 degrees, the beam spot was approximately 8 cm high by 2 cm wide. Since the range of 740 MeV protons in uranium is about 25 cm, the proton beam was stopped in the target. A helium-filled ion chamber integrated the total beam on the target. This chamber was calibrated by the Health Physics Division of LBL by placing a 1/16 - inch thick polethylene disk in front of the chamber and measuring the activity of carbon-11 produced by the (p, np) reaction. This calibration is known to $\pm$ 7 percent. Typical beam currents of from 1 to 3 nanoamperes were used for the neutron measurements.

As indicated in Fig. 11, two target positions were used to permit measurements at 50 and 130 degrees. The

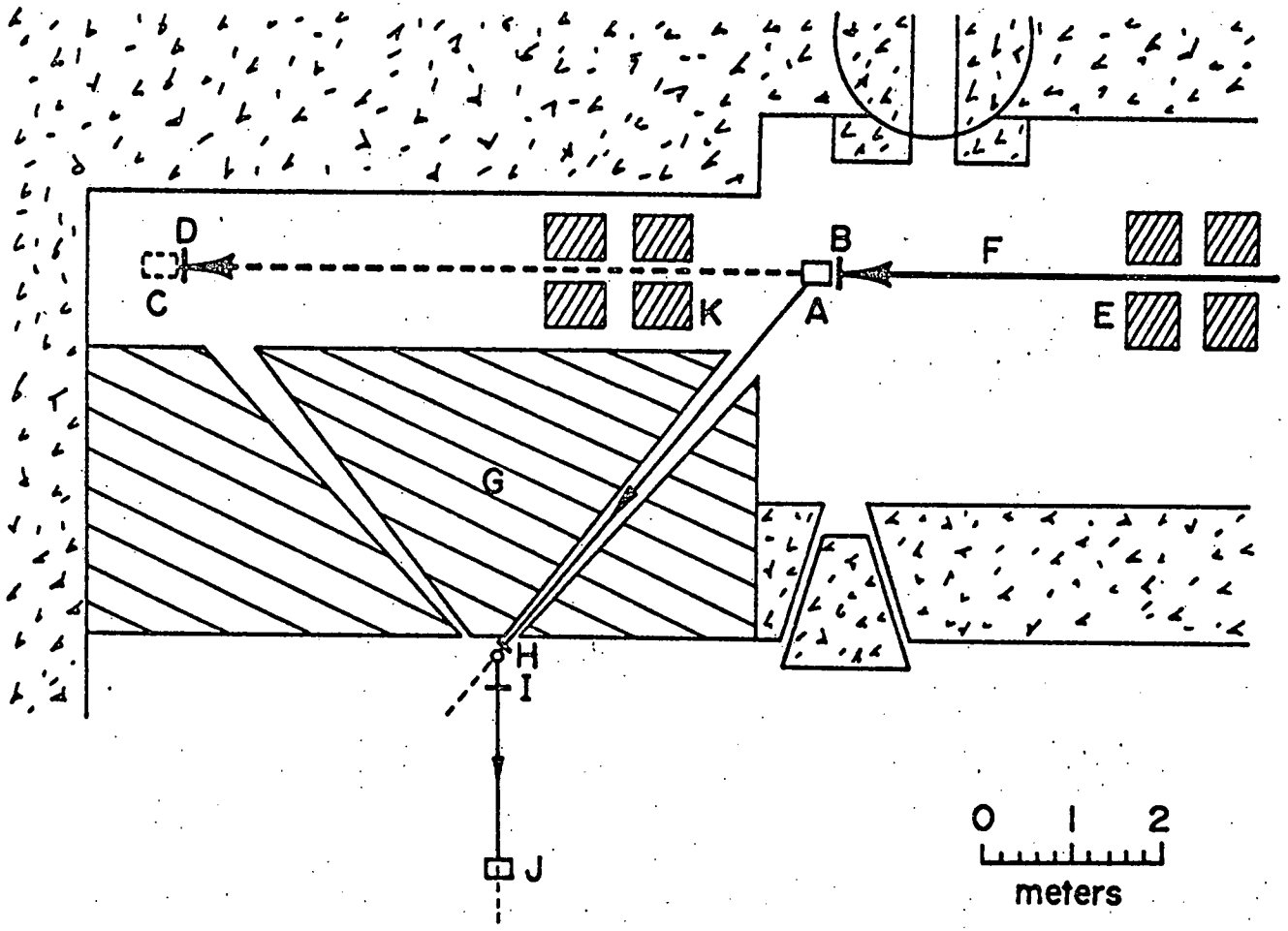

FIG. 11 Schematic diagram of the experimental set up at the LBL 184-inch cyclotron. (A) uranium-238 target in position for 50° measurement; (B) 50° ion-chamber position; (C) 130° target position; (D) 130° ion-chamber position; (E) 30-cm quadrupole magnet; (F) proton beam; (G) 20-cm high steel collimator; (H) A1 anti-coincidence and D1 detectors; (I) A2 anti-coincidence detector; (J) D2 detector; (K) 20-cm quadrupole magnet.

collimator consisted of a 20 cm thick steel plate assembled to the shape shown in Fig. 11 with reinforced concrete above and below the channel. The exit aperture of this collimator was approximately 7.6 cm wide by 20 cm high. The spectrometer configuration for the measurement at 50 degrees is shown schematically in Fig. 11.

3-3. Time-of-Flight Measurements

Three separate spectrum measurements were made: (1) from 20 to 500 MeV at 50 degrees, (2) from 1 to 15 MeV at 130 degrees, and (3) from 15 to 140 MeV at 130 degrees with respect to the proton beam. The neutron flight-path used for each of these measurements was selected to attain an energy resolution of between 10 and 20 percent for the range of energies measured. Small scintillators were used for the low-energy measurement at 130 degrees to avoid severe neutron attenuation and to reduce the plural scattering background. The scintillator dimensions for each measurement are listed in Table I. The mean neutron flight-path and scattering angle are listed in Table II. Separate measurements were made with NE-102 and NE-228 Dl scintillators for neutron energies above 15 MeV to permit subtraction of the background from

TABLE I. Scintillator dimensions used in the measurements from the thick uranium target.

Spectral Region		Scintillator Dimensions[(i)] in inches									
Observation angle Φ (deg)	Energy region T(MeV)	D1 cylinder		D2 cylinder		A1 slab			A2 slab		
		d	h	d	h	h	w	ℓ	h	w	ℓ
50	>20	4	4	9	8	4	4	$\frac{1}{4}$	4	4	$\frac{1}{2}$
130	1-15	1	1	4	2	4	4	$\frac{1}{4}$	6	6	$\frac{1}{4}$
130	>15	$2\frac{1}{2}$	$2\frac{1}{2}$	9	8	4	4	$\frac{1}{4}$	6	6	$\frac{1}{4}$

(i) height (h), diameter (d), width (w), thickness (ℓ)

TABLE II. The neutron flight-path and scattering angle in the measurements from the thick uranium target

Observation angle Φ (deg)	Energy region T(MeV)	Mean-neutron flight path X(cm)	Mean-neutron scattering angle θ (deg)
50	>20	300	40
130	1-15	98	39
130	15	226	39

neutron-carbon interactions. All other scintillators consisted of NE-102 plastic.

Figure 8 is an example of the data obtained in a time-of-flight measurement. Fig. 8(a) is a plot of the counts per channel versus the channel number for neutrons for 15 to 140 MeV at 130 degrees. This spectrum was measured with an NE-102 D1 scintillator; the measurement with an NE-228 scintillator is very similar in appearance and is not shown. In addition to the neutron time-of-flight spectrum, the spectrum of accidental coincidences was measured with a separate delayed coincidence channel. Figure 8 (b) is a plot of the spectrum of accidental coincidences which was measured simultaneously with the neutron time-of-flight spectrum shown in Fig. 8 (a). The number of events vetoed and the number of events veoted accidentally were also measured. The number of events vetoed accidentally was less than 1 percent.

Background time-of-flight measurements were made with the uranium target out of the beam at the beginning and conclusion of each measurement. With the target out, the number of background events was less than $\frac{1}{2}$ of 1

percent of the number of real events with the target in.

3-4. Analysis of the Time-of-Flight Data

Analysis of the time-of-flight data proceeds through four basic steps: (1) subtraction of the accidental coincidences, (2) time-of-flight and energy calibration of the spectrum, (3) subtraction of the carbon background, and (4) conversion to absolute units. Each of these steps is described briefly in the following paragraphs.

The level of accidental coincidences in the high-energy time-of-flight spectra was determined by performing a linear least-squares fit to the regions of accidental coincidences on both sides of the gamma-ray and neutron time-of-flight peaks. The channels selected for the least-squares fit were far enough removed from the gamma-ray and neutron peaks to avoid a contribution from "tails" of these spectra. The neutron time-of-flight peak in the low-energy measurement at 130 degrees extends to the right-hand edge of the spectrum; hence, the method described above could not be used. For this measurement, a least-squares fit

was made to the spectrum of accidental coincidences which was measured separately. This method is acceptable, but not preferred, because the spectrum of accidental coincidences is measured with a separate coincidence circuit.

The peak channel of the gamma-ray time-of-flight spectrum serves as a reference for determining the time-of-flight corresponding to each channel. The neutron energy corresponding to each channel of the spectrum was determined from the gamma-ray peak channel in the manner described in Section 2-7. After energy calibrating the spectrum, the data were regrouped into a histogram in which the bin widths are equivalent to the energy resolution of the spectrometer (fwhm) for the mean energy of the bin.

In order to subtract the carbon background, the spectrum measurements made with the NE-102 and NE-228 Dl scintillators were first normalized to the ion-chamber monitor and corrected for differences in scintillator volume and neutron attenuation. The two spectra were then combined in the algebraic expressions given by Eqs. (10) through (13) to determine the carbon background.

The carbon background in the time-of-flight spectra was extensive. The carbon background in the NE-102 measurement at 50 degrees varied from 39 percent in the interval from 20 to 25 MeV to 87 percent in the interval from 300 to 500 MeV. In the corresponding NE-228 measurement, the carbon background varied from 25 percent in the interval from 20 to 25 MeV to 78 percent in the interval from 300 to 500 MeV. In the spectrum shown in Fig. 8(a), the carbon background varied from 29 percent in the interval from 15 to 19 MeV to 85 percent in the interval from 97 to 138 MeV. In the corresponding time-of-flight spectrum measured with an NE-228 D1 scintillator, the carbon background varied from 18 percent in the interval from 15 to 19 MeV to 74 percent in the interval from 97 to 138 MeV. The carbon background in the spectra measured with the NE-228 D1 scintillator was less because of the higher hydrogen to carbon ratio. No significant carbon background was expected in the low-energy spectral measurement at 130 degrees; hence, the low-energy spectrum was measured only with an NE-102 D1 scintillator. The reasons for this expectation are twofold: (1) the carbon background produced by neutrons below

15 MeV is negligible; and (2) since the relative number of neutrons above 15 MeV is small, carbon background in the region from 5 to 15 MeV produced by neutrons above 15 MeV is expected also to be small. With regard to neutrons below 15 MeV, the inelastic carbon reaction $C(n,n'3\alpha)$ is the only energetically possible carbon reaction that produces a charged particle detectable in D1 and a secondary neutron detectable in D2; however, since the threshold for this reaction is 7.9 MeV and the cross-section is negligible below about 12 MeV, no significant background is expected. The importance of carbon background in the region from 5 to 15 MeV arising from higher energy neutrons depends upon the relative number of high-energy neutrons and also on the relative magnitude of the total inelastic carbon cross-section for high-energy neutrons. In the calculated spectrum above 5 MeV at 130 degrees, 50 percent of the neutrons are below 8 MeV, 67 percent below 10 MeV, 85 percent below 15 MeV, and 94 percent below 30 MeV. Since the cross-section for inelastic carbon reactions above 15 MeV remains a small fraction of the cross-section for elastic n-p scattering below 15 MeV, no significant background is expected in the 5 to 15 MeV

region from the small portion of the spectrum above 15 MeV.

The differential neutron yield $Y(T,\Omega)$ in units of neutrons/proton-MeV-steradian for each energy interval δT of the spectrum is given by the expression

$$Y(T,\Omega) = \frac{Xl^2 \delta R(T,\Omega,\theta)}{N_p n_H \Omega_2 V \varepsilon_2(T,\theta) \sigma(T,\theta)\, G(T,\theta) \delta T} \qquad (35)$$

here Xl is the distance between the centers of the target and Dl scintillator; $\delta R(T,\Omega,\theta)$ is the number of events observed in the energy interval δT centered at the incident neutron energy T; N_p is the total number of protons incident on the target during the measurement; n_H is the numerical density of hydrogen in the Dl scintillator; Ω_2 is the solid angle subtended by the D2 scintillator at the center of the Dl scintillator; V is the volume of the Dl scintillator; $\sigma(T,\theta)$ is the laboratory differential n-p scattering cross section for scattering a neutron with energy T through an angle θ; $G(T,\theta)$ is the total neutron attenuation factor for incident and scattered neutron in the Dl, Al, and A2 scintillators; $\varepsilon_2(T',\theta)$ is the neutron detection efficiency of the D2 detector for scattered neutrons with energy T'; and δT is the energy width of the

interval.

The energy-dependent terms (ε_2, σ, and G) in Eq. (35) were evaluated in the following manner:

(1) The neutron detection efficiency $\varepsilon_2(T,\theta)$ of the D2 detector was computed with a program written by Kurz (1964).

(2) For neutron energies below 22.5 MeV, values of the n-p differential cross section $\sigma(T,\theta)$ were obtained from the parameterization by Clements and Winsberg (1960). Above 22.5 MeV, the n-p differential cross sections were obtained from the parameterizations of Rindi et al. (1970). The equations for transforming the neutron scattering angles and the differential cross sections from the center-of-mass to the laboratory system were taken [Eqs. (30) and (34)] from Phillips and Thorton (1967).

(3) The total attenuation factor $G(T,\theta)$ was determined by integrating the attenuation factors g_1 and g_2 for the incident and scattered neutrons over the volume of the D1 detector as described in Section 2-5.2.

The spectrum measured at 50 degrees is listed in Table III. The spectra measured at 130 degrees for the low- and high-energy regions are listed in Tables IV and V, respectively. These tables list the energy interval, the energy resolution, and the absolute differential neutron yield. The uncertainty in the neutron yield listed in these tables represents the statistical uncertainty in the measurement.

Although the low-energy spectrum at 130 degrees was measured from 1 to 15 MeV, only the portion of the spectrum above 5 MeV is reported. The D2 discriminator bias level was calibrated to be at 50 keV (equivalent-electron energy); however, since the light output of electrons is nonlinear below about 100 keV, there is a large uncertainty in this calibration. The D2 detector efficiency below 5 MeV is sensitive to this uncertainty. Since the neutron spectrum in the region below 10 MeV has been measured by Veeser et al., further effort to interpret our results below 5 MeV does not seem worthwhile at this time.

3-5. Discussion of Uncertainties

The uncertainty in the absolute value of the neutron yield is estimated to be $\pm$ 15 percent at 130 degrees and $\pm$ 20

TABLE III. The absolute differential neutron yield at 50 degrees from 740 MeV proton bombardment of a 30-cm thick uranium-238 target and the energy resolution of the spectrometer computed for the mean energy of the interval.

Energy interval δT(MeV)	Energy resolution $\Delta T/T$ (%)	Absolute differential yield $Y(10^{-5}$ neutrons/proton-sr-MeV)
19.9 - 24.6	10.0	162 ± 9
24.6 - 30.3	10.3	127 ± 8
30.3 - 37.6	10.6	131 ± 8
37.6 - 46.8	11.0	128 ± 8
46.8 - 60.1	11.5	126 ± 8
60.1 - 77.9	12.1	100 ± 7
77.9 - 101.9	13.0	71 ± 6
101.9 - 140.0	14.3	49 ± 6
140.0 - 196.7	16.2	36 ± 5
196.7 - 302.0	19.2	16 ± 3
302.0 - 501.6	24.8	3 ± 2

TABLE IV. The absolute differential neutron yield from 5 to 15 MeV at 130 degrees from 740 MeV proton bombardment of a 30-cm thick uranium-238 target and the energy resolution of the spectrometer computed for the mean energy of the interval.

Energy interval δT(MeV)	Energy resolution $\Delta T/T$ (%)	Absolute differential yield $Y(10^{-3}$ neutron/proton-sr-MeV)
4.9 - 6.0	10.5	72 ± 4
6.0 - 7.6	10.9	38 ± 3
7.6 - 9.5	11.3	18 ± 3
9.5 - 12.1	11.9	9 ± 2
12.1 - 15.6	12.6	8 ± 2

TABLE V. The absolute differential neutron yield above 15 MeV at 130 degrees from 740 MeV proton bombardment of a 30-cm thick uranium-238 target and the energy resolution of the spectrometer computed for the mean energy of the interval.

Energy interval δT(MeV)	Energy resolution $\Delta T/T$(%)	Absolute differential yield $Y(10^{-5}$ neutron/proton-sr-MeV)
15.0 - 19.0	11.6	200 ± 9
19.0 - 24.2	11.9	130 ± 7
24.2 - 31.2	12.2	89 ± 7
31.2 - 40.6	12.7	64 ± 6
40.6 - 53.3	13.3	51 ± 6
53.3 - 70.8	14.1	30 ± 5
70.8 - 96.9	15.2	9 ± 5
96.9 - 138.0	16.9	3 ± 4

percent at 50 degrees. These estimates were determined from the considerations listed below. (1) Kurz (1964) estimates the uncertainty in the neutron detection efficiency $\varepsilon_2(T')$ to be $\pm$ 10 percent. (2) The uncertainty in the ion-chamber monitor calibration is $\pm$ 7 percent. (3) The uncertainty in the differential n-p cross section $\sigma(T,\Theta)$ is estimated to be $\pm$8 percent. (4) The attenuation factor G(T) is based on the total n-p and n-C cross sections which are known to about $\pm$ 5 percent; however, approximations in the computational technique increase this uncertainty to an estimated $\pm$ 8 percent. (5) In the measurement at 50 degrees, the fact that the D1 scintillator was not fully illuminated resulted in an estimated uncertainty of $\pm$ 10 percent in the D1 scintillator volume. The illuminated volume was computed from the geometry of the experimental arrangement.

Veeser et al. (1972, 1973) calculated the contribution to the neutron beam from neutrons scattered in the collimator walls. The results of this Monte Carlo calculation indicate that for neutron energies between 0.1 and 14 MeV there is a contribution to the neutron beam of between 2.5 and 3 percent. Sufficient cross sction data does not exist to perform this

calculation at higher energies. Since this correction is small, no correction was made to the data.

A small percentage of the real events were "blocked" by accidental coincidences. In the measurement at 50 degrees, about 1.5 percent of the real events were lost on this account; in the measurements at 130 degrees about 0.25 percent of the events were lost. Since these losses were small, no corrections were made to the data.

There is background in the measured spectrum as a result of neutrons scattering into the D2 detector from second or higher-order interactions in the D1 detector. As described in Section 2-4.3, the plural scattering background is expected to be more significant in the lower energy portion of a measured spectrum. Also, the percentage of the background in the low-energy region is expected to be larger in a spectrum in which the number of neutrons increases with energy than in a spectrum in which the number of neutrons decreases with energy. An experimental measurement of the plural scattering background was made by measuring the high-energy spectrum at 130 degrees with D1 scintillators of significantly different diameter. Although the uncertainty in this measurement was large, we were able

to place an upper limit of about 12 percent on the plural scattering background in the low-energy region of the spectrum. The actual plural scattering backgrounds in the low-energy regions of the spectra are estimated to be about 5 percent from the following considerations: (1) In each measurement, the diameter of the D1 scintillator was less than the mean-free-path for the lowest neutron energy recorded, and (2) each spectrum decreased steeply with increasing neutron energy. We estimate that the plural scattering background is negligible for neutron energies above 75 MeV in the measurement at 50 degrees; above 50 MeV in the high-energy measurement at 130 degrees; and above 7 MeV in the low-energy measurement at 130 degrees. The reason is that for neutrons above these energies, the mean-free-path for nuclear interactions is several times greater than the diameter of the D1 scintillator.

3-6. Comparison with Monte Carlo Calculations

The neutron spectra measured at both 50 and 130 degrees are plotted in Fig. 12. For comparison, the calculated spectra averaged over the intervals from 33.5 to 60 degrees and from 120 to 146.5 degrees are shown as histograms. These spectra were calculated by Fullwood et al. (1972) for 800 MeV protons on

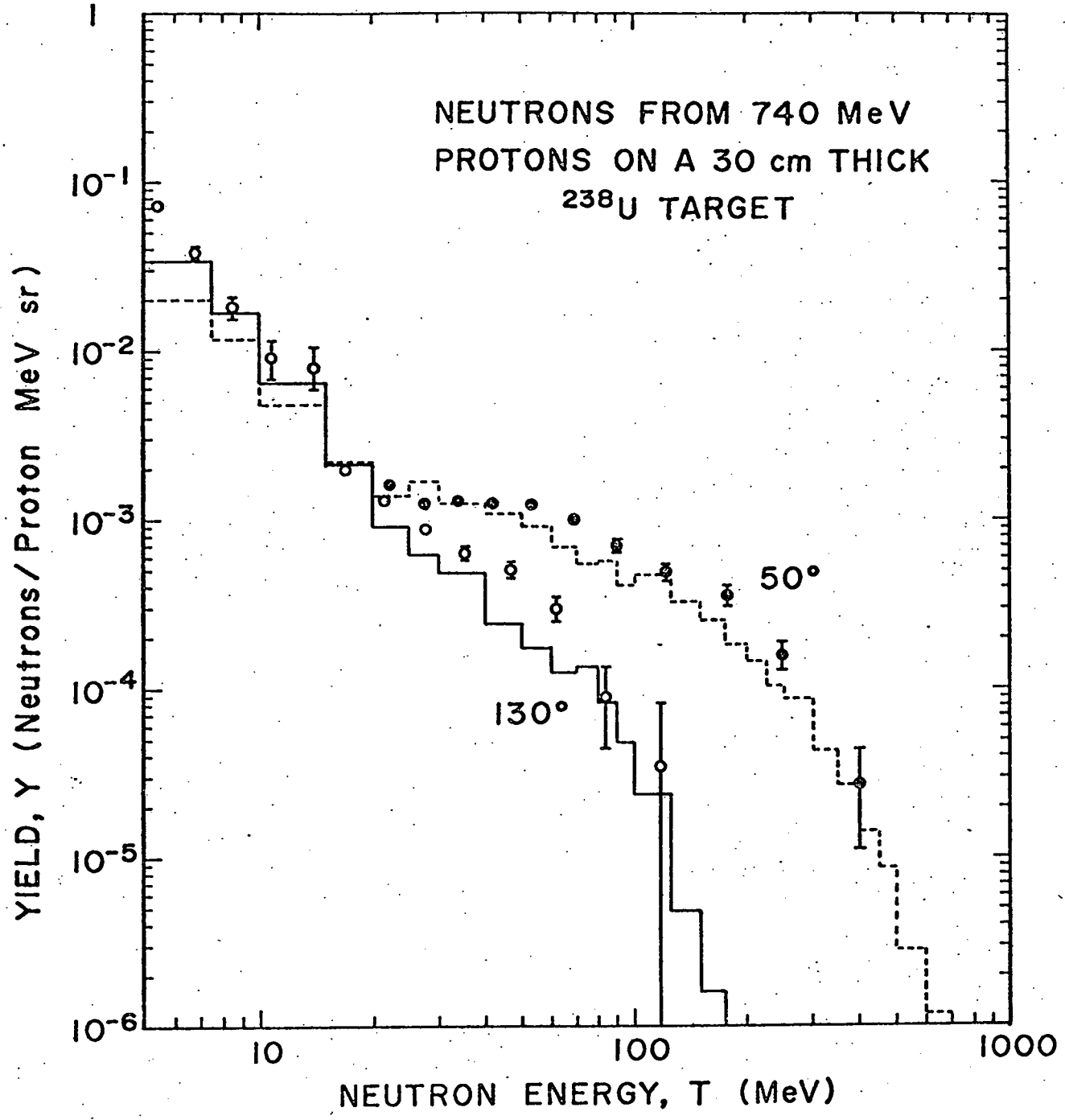

FIG. 12 Experimental and calculated neutron yields at both 50° and 130° from 740 MeV proton bombardment of a 30-cm thick uranium-238 target. The histogram shows the calculated results for 800 MeV protons averaged over the angular intervals from 33.5 to 60° and from 120 to 146.5°.

a uranium target of the same dimensions using the nucleon-meson transport code NMTC written by Coleman (1970). This code computes the transport of particles down to a cutoff energy of 25 MeV. A second code, the Monte Carlo neutron transport code MCN written by Cashwell (1972) was used to transport neutrons below 25 MeV out of the target. The shape of the experimental and calculated spectra are in good agreement and the forward peaking of the cascade neutrons is clearly evident.

Although the calculation of Fullwood et al. (1972) was made for 800 MeV protons on the target axis, the proton beam energy in the experiment was actually 740 MeV and the beam profile was elliptical. In order to determine the effect of these differences on the calculated spectra above 25 MeV, Seeger (1972) reran the NMTC calculation for 740 MeV protons with an elliptical (2 cm by 8 cm) beam profile. The effect of these differences was small. The differential yield of neutrons above 25 MeV decreased by about 6 percent at 50 degrees and by about 3 percent at 130 degrees. A calculated decrease of 8 percent in the number of neutrons produced per incident proton at 740 MeV reflects the 8 percent decrease in beam energy from 800 MeV to 740 MeV. This decrease was most pronounced in the forward direction.

Seeger did not calculate the low-energy spectra (< 25 MeV).

Below 20 MeV, the measurements are in agreement with the Monte Carlo calculation; the data point at 5.4 MeV is in agreement with the calcuated spectrum at 5 MeV. Above 25 MeV, the neutron yield at 50 degrees is 1.4 times that calcuated for 740 MeV protons; at 130 degrees, this factor increases to 1.6. At 50 degrees, the measured yield of neutrons above 25 MeV is 5 times greater than that at 130 degrees. From the measurements at 50 and 130 degrees, it is estimated that the total integrated yield above 25 MeV is 0.9_5 neutrons per incident proton; the Monte Carlo calculation predicts 0.67 neutrons above 25 MeV per incident 740 MeV proton.

A tendency for the magnitude of the calculated spectrum to fall below the measured spectrum as the angle of observation is increased has been noted in previous experiments with heavy metal targets. As noted in Section 3-1, the agreement between the data of Fraser et al. (1966) and the calculated spectrum is good at 45 degrees, fair at 90 degrees, and poor at 135 degrees. We estimate from examination of Fig. 6 in reference 4 that the measured yield at 135 degrees is a factor

of 3 greater than calculated. Bertini (1969) has compared the proton spectra of Azhgirey et al. (1959) from 660 MeV protons on a 7.62 g/cm^2 uranium target with the predictions of the intranuclear cascade calculation. Comparisons were made at 12, 18, and 30 degrees; agreement at all but the widest angle is good. At 30 degrees, the magnitude of the measured spectrum is greater than the calcuated spectrum. Bertini (1972) suggests that the tendency for the magnitude of the measured spectra to increase over the calculated spectra as the angle of observation is increased may be a result of interactions with clusters of nucleons (e.g., deuterons and alpha particles) in the nucleus which are not included in the code. An attempt to include these interactions into the code was carried out at Oak Ridge in connection with data at 60 MeV; in this case the computations indicated a contribution in the backward direction.

4. SUMMARY AND CONCLUSIONS

The research program in energetic-neutron spectrometry conducted under Contracts AT(30-1)-3914 and AT(11-1)-3258 with Clarkson College of Technology achieved success in developing a time-of-flight spectrometer for neutrons from 1 to 500 MeV and in measuring neutron spectra from a thick uranium target bombarded by 740 MeV protons from the 184-inch cyclotron of the Lawrence Berkley Laboratory.

The spectrometer developed represents a significant advance in neutron spectroscopy. Since the spectrometer is self-contained, and requires a relatively short flight-path of from 1 to 5 meters, it is readily adaptable to experiments at a variety of accelerators. The intrinsic time dispersion of the system with a $2\frac{1}{2}$ inch diameter by $2\frac{1}{2}$ inch high first detector and a 9 inch diameter by 8 inch thick second detector is 2.2 nsec (fwhm). For a 4 meter flight-path, the energy resolution varies from about 7 to 20 percent and the spectrometer efficiency varies from about 2×10^{-5} to 8×10^{-7} over the range of energies from 10 to 500 MeV. Measurements at 14 MeV confirm the resolution and efficiency of the spectrometer at low energies. Measurements at 220 MeV verify the

resolution of the spectrometer at this energy and demonstrate the technique for subtracting the carbon background.

Neutron spectra from 740 MeV proton bombardment of a 30-cm thick uranium target were measured from 20 to 500 MeV at 50 degrees and from 5 to 140 MeV at 130 degrees with respect to the proton beam at the 184-inch cyclotron of the Lawrence Berkeley Laboratory. The results are compared with the predictions of the nucleon-meson transport code NMTC based on the intranuclear cascade model. These comparisons show that the intranuclear cascade model underestimates the neutron production for cascade neutrons at wide angles; furthermore, these comparisons show that this discrepancy increases with increasing angle of emission. This discrepancy may be due to interactions with clusters of nucleons (e. g., deuterons and alpha particles) in the nucleus which are not taken into account in the intranuclear cascade model. Specifically, the following conclusions can be made from comparison of the calculated and measured spectra:

1. The shapes of the measured and calculated spectra are in general agreement.
2. Below 20 MeV, the results are in agreement with the calculation.

3. For neutrons above 25 MeV, the measured yield at 50 degrees is 5 times greater than that at 130 degrees.
4. At 50 degrees, the yield of neutrons above 25 MeV is 1.4 times that calculated; at 130 degrees, this factor increase to 1.6.
5. From the measurements at 50 and 130 degrees, it is estimated that the total integrated yield above 25 MeV is 0.9_5 neutrons per incident proton; whereas, the calculation predicts 0.67 neutrons per incident proton.

REFERENCES

ALSMILLER, R. G., Jr.
1969: and J. W. Wachter and H. S. Moran, "Calculation of the Neutron and Proton Spectra from Thick Targets bombardment by 450-MeV Protons and Comparison with Experiment," Nucl. Sci. and Eng. 36, 291.

AZHGIREY, L. S.
1959: and I. K. Vzorov, V. P. Zrelov, M. G. Mescheryakov, B. S. Neganov, R. M. Ryndin, and A. G. Shabudin, "Nuclear Interactions of 660 MeV Protons and the Momentum Distribution of Nucleons in Nuclei," Nucl. Phys. 13, 258.

BALDWIN, A.
1971: "A Gated Pulse-Shape-Discrimination System for High Data Acquisition Rates," M. S. Thesis, Clarkson College of Technology.

BERTINI, H. W.
1963: "Low-Energy Intranuclear Cascade Calculation," Phys. Rev. 131, 1801.

1965: Erratum to 1963 paper, Phys. Rev. 138, AB2.

1967: "Secondary Particle Spectra from the Interaction of 30- to 340-MeV Protons on Complex Nuclei: Experimental Data and Comparison with Theory," Phys. Rev. 162, 976.

1969: "Intranuclear-Cascade Calculation of the Secondary Nucleon Spectra from Nucleon-Nucleus Interactions in the Energy Range 340 to 2900 MeV and Comparisons with Experiment," Phys. Rev. 188, 1711.

1972: private communication.

BRADY, F. P.
1968: and J. A. Jungerman, J. C. Young, J. L. Romero, and P. J. Symonds, "Detection Efficiency of a Plastic Scintillator for 10-70 MeV Neutrons," Nucl. Instr. and Meth. 58, 57; Erratum, Nucl. Instr. and Meth. 63, 358.

CASHWELL, E. D.
1972: and G. D. Turner, Los Alamos Scientific Laboratory Report LA-4751.

CLEMENTS, T. P.
1960: and L. Winsberg, "Polynomial Fits of Nucleon-Nucleon Scattering Data," University of California Radiation Laboratory Report UCRL-9043.

COLEMAN, W. A.
1970: and T. W. Armstrong, "The Nucleon-Meson Transport Code NMTC," Oak Ridge National Laboratory Report ORNL-4606.

CRABB, D. G.
1967: and J. G. McEwen, E. G. Auld, and A. Langsford, Nucl. Instr. and Meth. 48, 87.

FRASER, J. S.
1966: and J. S. Hewitt, and J. Walker, "Neutron Spectra and Angular Distribution Produced by 1 GeV Protons on a Thick Lead Target," Physics in Canada L2 (2), 62 (1966).

FULLWOOD, R. R.
1972: and J. D. Cramer, R. A. Haarman, R. P. Forrest, Jr., and R. G. Schrandt, "Neutron Production by Medium-Energy Protons on Heavy Metal Targets," Los Alamos Scientific Laboratory Report LA-4789.

GOODING, T. J.
1960: and H. G. Pugh, "The Response of Plastic Scintillators to High Energy Particles, "Nucl. Instr. and Meth. 7, 189.

1961: Erratum to 1960 paper, Nucl. Instr. and Meth. 11, 365.

HADLEY, J.
1949: and E. Kelly, C. Leith, E. Segre, C. Wiegand, and H. York, "Experiments on n-p Scattering with 90- and 40-MeV Neutrons," Phys. Rev. 75, 351.

HANSON, A. O.
1947: and J. L. McKibben, Phys. Rev. 72, 673.

KURZ, R. J.
1964: "A 709/7090 FORTRAN II Program to Compute the Neutron-Detection Efficiency of Plastic Scintillator for Neutron Energies from 1 to 300 MeV," University of California Radiation Laboratory Report UCRL-11339.

MADEY, R.
1968a: "An Energetic-Neutron Spectrometer," IEEE Transactions on Nuclear Science NS-15 (3), 426.

1968b: "A Spectrometer for Neutrons from 10 to 100 MeV," Proceedings of the International Symposium on Nuclear Electronics and Radioprotection, Toulouse, France (4-8 March).

1968c: "A Time-of-Flight Spectrometer for Neutrons from 10 to 100 MeV," Bull. Am. Phys. Soc. 13 (1), 51.

1972: and F. M. Waterman, "The Response of NE-228 Scintillator to 3.5, 5.8, and 10.5 MeV Protons," Nucl. Instr. and Meth. 104, 253.

OSBORN, D. H.
1969a: and R. Madey, "Neutron Spectrometer Performance at 14 MeV," Proceedings of the Second International Conference on Accelerator Dosimetry and Experience, CONF-691101, Stanford Linear Accelerator Center, Stanford, California (5-7 November).

1969b: and R. Madey, "Neutron Spectrometer Performance at 14 MeV," Bull. Am. Phys. Soc. 14 (12), 1214.

PHILLIPS, R. E.
1967: and S. T. Thornton, "A Fortran Program for Relativistic Kinematic Calculations in Two-Body Nuclear Reactions," Oak Ridge National Laboratory Report ORNL-4179.

RINDI, A.
1970: and C. B. Lim, and T. Salmon-Cinotti, "(n, p) Elastic Scattering: A Fitting Expression for the Differential Cross Sections in the Energy Range Between 22.5 and 400 MeV," University of California Radiation Laboratory Report UCRL-20295.

SEEGER, P. A.
1972: Private Communication.

SERBER, R.
1947a: "The Production of High Energy Neutrons by Stripping," Phys. Rev. 72, 1008.

1947b: "Nuclear Reactions at High Energies," Phys. Rev. 72, 1114.

VEESER, L. R.
1972: and E. R. Shunk, A. A. Robba, and R. R. Fullwood, "Low-Energy Neutrons Produced by 740-MeV Protons on Uranium," Los Alamos Scientific Laboratory Report LA-DC-13031.

1973: and R. R. Fullwood, A. A. Robba, and E. R. Shunk, "Neutrons Produced by 740-MeV Protons on Uranium," Los Alamos Scientific Laboratory Report LA-UR 73-768 (to be published).

VERBINSKI, V. V.
1968: and W. R. Burrus, T. A. Love, W. Zobel, N. W. Hill, and R. Textor, "Calibration of an Organic Scintillator for Neutron Spectrometry," Nucl. Instr. and Meth. 65, 8.

WACHTER, J. W.
1967: and W. R. Burrus, and W. A. Gibson, "Neutron and Proton Spectra from Targets Bombarded by 160-MeV Protons," Phys. Rev. 161, 971.

1972: and W. B. Gibson, and W. R. Burrus, "Neutron and Proton Spectra From Targets Bombarded by 450-MeV Protons," Phys. Rev. 6c, 1496 (1972).

WATERMAN, F. M.
1970: and D. H. Osborn, P. J. McNulty, and R. Madey, "Neutron Spectrometer Studies at 14 MeV," Bull. Am. Phys. Soc. 15 (4), 599.

1973: "High-Energy Neutrons Produced by 740-MeV Protons on Uranium," Ph. D. Dissertation, Clarkson College of Technology.

WEIGAND, C. E.
1962: and T. Eliott, W. B. Johnson, L. B. Auerbach J. Lach, and T. Ypsilantis, Rev. Sci. Instr. 33 , 526.

YOUNG, J. C.
1968: and J. L. Romero, F. P. Brady, and J. R. Morales, "Detection Efficiency of a Plastic Scintillator for 20 to 170 MeV Neutrons," Nucl. Instr. and Meth. 68, 333.